



Mineral Liberation Analysis

Porphyry copper Report

Submitted by:

Mody Oury Barry – 67682

Master's Program:

Sustainable Mining and Remediation Management

Lecturer:

Pr. Dr. Bernhard Schulz

Date: 10.09.24

Report Overview:

This report is based on analysis from four measurement zip files of samples collected from a flotation mineral processing line for porphyry copper ore. The analysis employs both MLA (Mineral Liberation Analysis) Views and Data Views to address the following objectives:

This report is based on the analysis of four measurement zip files from samples taken from a flotation mineral processing line of porphyry copper ore. The analysis employs both MLA (Mineral Liberation Analysis) Views and Data Views to address the following objectives:

1. Data View File Preparation:

- Shortening file names of the *.mdb data files for easier management.
- Extracting mineral reference data from a sample in the MLA DataView database to obtain key properties such as density, chemical formulas, and elemental composition.

2. Mineral Description:

- Describing copper sulfide, pyrite, and molybdenite particles in both concentrate and tailing samples.

3. Grouping and Diagram Preparation:

- Creating a convenient grouping list with copper minerals categorized together in the MLA database.
- Preparing diagrams showing cumulative grain size distribution curves for copper minerals (grouped together), pyrite, quartz, feldspar, and mica from concentrate and the tailing with the lowest copper mineral content.
- Preparing grain size histograms for the same minerals from the concentrate.
- Describing the corresponding grain size histograms.

4. Grain Size Filtering and Analysis:

- Executing electronic filtering of the concentrate and tailings based on EC diameter.
- Defining three convenient grain size classes using the cumulative particle grain size distribution curve.

5. Comparative Description:

- Providing a comparative analysis of modes and mineral liberation, including Particle Composition and Free Surface, for both unfiltered and filtered subsamples from all samples.

Table of Contents

Introduction.....	1
1. Data View file Preparation.....	1
1.1. Shortening the file names of the *.mdb data files accordingly	1
2. Description of the copper sulfide, the pyrite, and the molybdenite particles in concentrate and tailing	3
2.1. Description of the different mineral particles	5
2.1.1. Chalcopyrite.....	5
2.1.2. Pyrite.....	6
2.1.3. Molybdenite	8
2.1.4. Bornite.....	10
2.1.5. Chalcocite	12
2.1.6. Covellite.....	14
3. Preparing a shorter and convenient grouping list with copper minerals grouped together in the *mla database.....	17
4. Preparing diagrams with the cumulative grain size distribution curves for copper minerals (grouped together), pyrite, quartz, feldspar, and mica from concentrate and the tailing with the lowest content of copper minerals	19
4.1. Grain size distribution curve for copper minerals in both the concentration (V3-SP1) and the tailing (V3-RS1).....	19
4.2. Grain Size distribution curve for pyrite in both the concentrate (V3-SP1) and the tailing (V3-RS1).....	22

4.3. Grain size distribution curve for Quartz in both the concentrate (V3-SP1) and tailing (V3-RS1).....	25
4.4. Grain distribution curve for feldspar in the concentrate (V3-SP1) and the tailing (V3-RS1).....	28
4.5. Grain size distribution curve for mica in both the concentrate (V3-SP1) and the tailing (V3-RS1).....	31
5. Preparing corresponding grain size histograms for copper minerals (grouped together), pyrite, quartz, feldspar, and mica from the concentrate	34
5.1. Description of the corresponding grain size histograms	35
6. Execution of an electronic filtering of the concentrate and tailings through EC diameter. Definition of three convenient grain size classes for this filtering by using the cumulative particle grain size distribution cure.....	36
7. Giving a text with a comparative description of modes and mineral liberation (Particle Composition and Free Surface) of unfiltered and filtered subsamples from all samples.	40
7.1. Mineral liberation by particle composition	40
7.2. Mineral liberation by particle surface	46
8. Reference	52

List of Figures

Figure 1. Files renamed in MLA DataView.....	1
Figure 2.Modal Mineralogy of the concentrate (V3-SP1, SP3, SP4) and tailing (V3-RS1).....	3
Figure 3. Minerals distribution in the Concentrate (V3-SP1) at a scale of 150 μm	4
Figure 4. Minerals distribution in the tailing (V3-RS1) at a scale of 150 μm	4
Figure 5. Chalcopyrite Particles in Concentrate V3-SP1 at scale of 200 μm	5
Figure 6. Chalcopyrite grain mantled with Chalcocite and Bornite in V3-SP1 at scale of 20 μm	6
Figure 7. Chalcopyrite particles in tailing V3-RS1 at scale of 200 μm	6
Figure 8. Pyrite particles in concentrate V3-SP1 at scale of 200 μm	7
Figure 9.Pyrite particle mantled with some minerals mentioned in the legend in V3-SP1 at a scale of 20 μm	8
Figure 10.Pyrite particle distribution in tailing V3-RS1 at a scale of 100 μm	8
Figure 11. Molybdenite particles distribution in tailing V3-RS1at a scale of 200 μm	9
Figure 12. Molybdenite particles distribution in tailing V3-RS1 at a scale of 200 μm	10
Figure 13. Bornite particles distribution in concentrate V3-SP1 at a scale of 200 μm	11
Figure 14. Bornite particle mantled with quartz in concentrate V3-SP1 at a scale of 20 μm	12
Figure 15. Bornite particles distribution in tailing V3-RS1 at a scale of 200 μm	12
Figure 16. Chalcocite particles distribution in concentrate V3-SP1 at a scale of 200 μm	13
Figure 17. Chalcocite particle occurring with Chalcopyrite particle in concentrate V3-SP1 at scale of 20 μm	14
Figure 18. Chalcocite particles occurring in tailing V3-RS1 at a scale of 200 μm	14
Figure 19. Covellite particles distribution in concentrate V3-SP1 at a scale of 200 μm	15
Figure 20. Covellite particle occurring with Chalcopyrite and Bornite particles in concentrate V3-SP1 at a scale of 10 μm	16
<i>Figure 21. Covellite particles occurring in the tailing V3-RS1 at a scale of 200 μm.....</i>	16
Figure 22. Minerals grouped by type.....	17

Figure 23. grouping of minerals, highlighting the grouping of copper-bearing minerals within the different concentrates (V3-SP1, SP3, SP4) and the tailing (V3-RS1) in MLA DataView	18
Figure 24. Copper minerals grain size distribution cure for the concentrate (V3-SP1) and the tailing (V3-RS1)	19
Figure 25. Grain size distribution curve for copper minerals in the concentrate (V3-SP1).....	20
Figure 26. Grain size distribution curve for copper minerals in the tailing (V3-RS1).....	21
Figure 27. Grain size distribution curve for pyrite in the concentrate (V3-SP1) and the tailing (V3-RS1).....	22
<i>Figure 28. Grain size distribution curve for pyrite in the concentrate (V3-SP1)</i>	23
Figure 29. Grain size distribution curve for pyrite in the tailing (V3-RS1).....	24
Figure 30. Grain size distribution curve for quartz in both the concentrate V3-SP1 and the tailing (V3-RS1)....	25
<i>Figure 31. Grain size distribution curve for quartz in the concentrate (V3-SP1)</i>	26
<i>Figure 32. Grain size distribution curve for quartz in the tailing (V3-RS1).....</i>	27
Figure 33. Grain size distribution curve for feldspar in the concentrate (V3-SP1) and the tailing (V3-RS1)	28
Figure 34. Grain size distribution curve for feldspar in the concentrate (V3-SP1).....	29
Figure 35. Grain size distribution curve for feldspar in the tailing (V3-RS1)	30
Figure 36. Grain size distribution curve for mica in the concentrate (V3-SP1) and the tailing (V3-RS1)	31
Figure 37. Grain size distribution curve for mica in the concentrate (V3-SP1).....	32
Figure 38. Grain size distribution curve for mica in the tailing (V3-RS1)	33
Figure 39. Cu_Sulfides grain size histogram in the concentrate V3-SP1	
histogram in the concentrate V3-SP1	34
Figure 40. Pyrite grain size	
Figure 41. Quartz grain size histogram.....	34
Figure 42. Feldspar grain size histogram.....	35
Figure 43. Mica grain size histogram	35
Figure 44. filtered (00-15 µm) particle size distribution curve for the concentrate (V3-SP1) and the tailing (V3-RS1).....	36

Figure 45. filtered (15-80 μm) particle size distribution curve for the concentrate (V3-SP1) and the tailing (V3-RS1).....	37
Figure 46. filtered (80-300 μm) particle size distribution curve for the concentrate (V3-SP1) and the tailing (V3-RS1).....	38
<i>Figure 47. Filtered (00-15 μm; 80-300 μm) modal mineralogy for V3-SP1; V3-SP3; V3-SP4</i>	39
Figure 48. Unfiltered mineral liberation by particle composition with samples, including V3-SP1, V3-SP3, V3-SP4, V3-RS1.....	41
Figure 49. mineral liberation by particle composition with samples, including V3-SP1, V3-SP3, V3-SP4, V3-RS, filtered at 00-15 μm	42
Figure 50. mineral liberation by particle composition with samples, including V3-SP1, V3-SP3, V3-SP4, V3-RS, filtered at 15-80 μm	43
Figure 51. mineral liberation by particle composition with samples, including V3-SP1, V3-SP3, V3-SP4, V3-RS, filtered at 80-300 μm	44
Figure 52. Unfiltered mineral liberation by free surface with samples, including V3-SP1, V3-SP3, V3-SP4, V3-RS1	47
Figure 53. Mineral liberation by free surface with samples, including V3-SP1, V3-SP3, V3-SP4, V3-RS1 filtered at 00-15 μm	48
Figure 54. Mineral liberation by free surface with samples, including V3-SP1, V3-SP3, V3-SP4, V3-RS1 filtered at 15-80 μm	49
<i>Figure 55. Mineral liberation by free surface with samples, including V3-SP1, V3-SP3, V3-SP4, V3-RS1 filtered at 80-300 μm</i>	50

List of Tables

Table 1. Mineral Reference.....	2
---------------------------------	---

Introduction

This report is based on four measurement zip files from samples taken from a flotation mineral processing line of porphyry copper ore. The analysis utilizes both MLA (Mineral Liberation Analysis) Views and Data Views to address the following questions.

1. Data View file Preparation

1.1. Shortening the file names of the *.mdb data files accordingly

The four files include:

V3-RS1-XBSE-SPX-brk-1-S-t2-t3-g-clr.mdb;

V3-SP1-XBSE-SPX-brk-1-S-t2-t3-g-clr.mdb

V3-SP3-XBSE-SPX-brk-1-S-t2-t3-g-clr.mdb

V3-SP4-XBSE-SPX-brk-1-S-t2-t3-g-clr.mdb

The following files will be renamed as follows:

V3-RS1-XBSE-SPX-brk-1-S-t2-t3-g-clr.mdb ==> V3-RS1

V3-SP1-XBSE-SPX-brk-1-S-t2-t3-g-clr.mdb ==> V3-SP1

V3-SP3-XBSE-SPX-brk-1-S-t2-t3-g-clr.mdb ==> V3-SP3

V3-SP4-XBSE-SPX-brk-1-S-t2-t3-g-clr.mdb ==> V3-SP4

This is illustrated in Figure 1 below

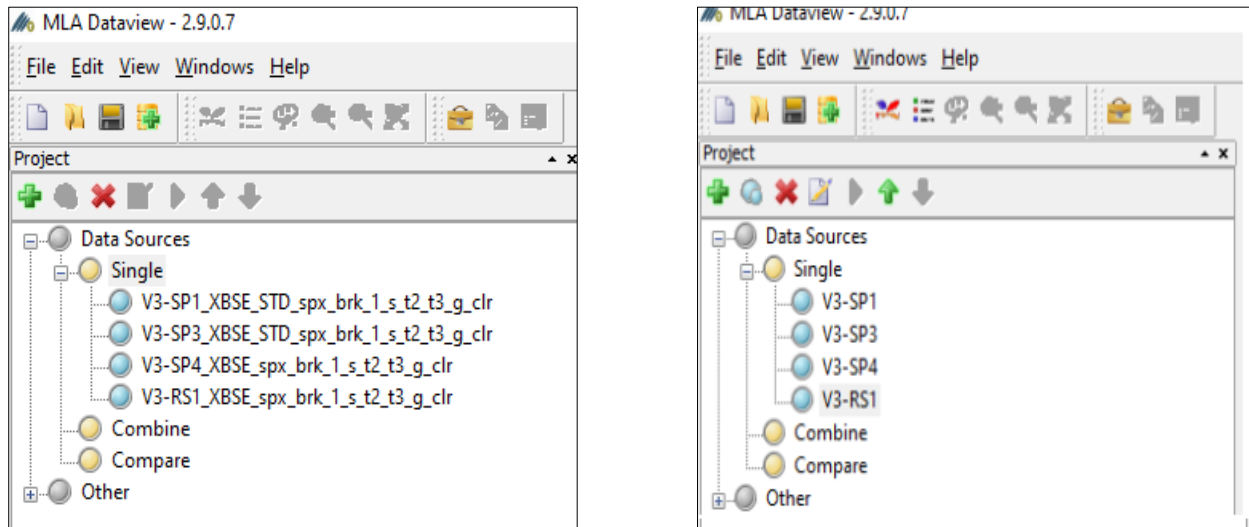


Figure 1. Files renamed in MLA DataView

After renaming the files, it is crucial to extract the mineral reference data from a single sample in the MLA DataView database. This provides valuable insights into key mineral properties, such as density, chemical formulas, and elemental composition, all of which are essential for the calculations.

'Calculation: Mineral Reference'																					
Type: Single																					
Mineral	Densi	Formula	Al (%)	As (%)	C (%)	Ca (%)	Cu (%)	F (%)	Fe (%)	H (%)	K (%)	Mg (%)	Mo (%)	O (%)	P (%)	Pb (%)	S (%)	Si (%)	Ti (%)	Zn (%)	
Bornite	5.07	Cu ₅ FeS ₄		0	0	0	0	63.314	0	11.129	0	0	0	0	0	0	25.558	0	0	0	
Chalcocite	5.7	Cu ₂ S		0	0	0	0	79.854	0	0	0	0	0	0	0	0	20.146	0	0	0	
Chalcopyrite	4.2	CuFeS ₂		0	0	0	0	34.626	0	30.431	0	0	0	0	0	0	34.943	0	0	0	
Covellite	4.7	CuS		0	0	0	0	66.464	0	0	0	0	0	0	0	0	33.536	0	0	0	
Pyrite	5	FeS ₂		0	0	0	0	0	0	46.549	0	0	0	0	0	0	53.451	0	0	0	
Molybdenite	4.8	MoS ₂		0	0	0	0	0	0	0	0	0	0	59.937	0	0	0	40.063	0	0	0
Galena	7.5	PbS		0	0	0	0	0	0	0	0	0	0	0	0	0	87	13	0	0	0
Sphalerite	4	ZnS		0	0	0	0	0	0	0	0	0	0	0	0	0	32.908	0	0	67.09	0
As-Cu-Co-Bi-Ni-Sulf	4.5	Cu ₃ AsS ₃		0	20.711	0	0	52.699	0	0	0	0	0	0	0	0	26.591	0	0	0	0
Quartz	2.65	SiO ₂		0	0	0	0	0	0	0	0	0	0	0	53.3	0	0	0	46.7	0	0
Feldspars	2.57	KAlSi ₃ O ₈	9.693529264	0	0	0	0	0	0	0	14.048	0	0	45.986	0	0	0	30.273	0	0	0
Biotite	3	K(Mg/Fe)3(AlSi ₃ O ₁₀)	6.3557	0	0	0	0	0	13.156	0.4749	9.2109	5.7268	0	45.227	0	0	0	0	19.849	0	0
Chlorite	3	(Mg ₃ Fe ₂)Al(AlSi ₃)C	8.719	0	0	0	0	0	18.048	1.303	0	11.784	0	46.532	0	0	0	0	13.614	0	0
Muscovite	2.8	KAl ₂ (AlSi ₃ O ₁₀) ₂	20.321	0	0	0	0	0	0.506	9.817	0	0	48.202	0	0	0	0	21.154	0	0	0
Other-Silicates	3.4	Ca ₂ (Al/Fe)3Si ₃ O ₁₂ OH	11.167	0	0	16.589	0	0	11.557	0.2086	0	0	0	43.042	0	0	0	0	17.437	0	0
Carbo-Sulfates	2.32	CaSO ₄ · 2H ₂ O		0	0	0	23.279	0	0	2.3419	0	0	0	55.755	0	0	18.623	0	0	0	0
Phosphates	3.2	Ca ₅ (PO ₄) ₃ F		0	0	0	39.739	0	3.7672	0	0	0	0	38.07	18.424	0	0	0	0	0	0
Fe-Oxides	5.26	Fe ₂ O ₃		0	0	0	0	0	69.944	0	0	0	0	30.056	0	0	0	0	0	0	0
Accessories	3.5	CaTiSiO ₅		0	0	0	20.443	0	0	0	0	0	0	0	40.801	0	0	0	14.325	24.431	0
Invalid	2.23	C		0	0	100	0	0	0	0	0	0	0	0	0	0	0	0	0	0	0

Table 1. Mineral Reference

Based on the modal mineralogy of the porphyry copper samples from the MLA DataView, as illustrated in Figure 2, it is evident that sample SP1 shows a high concentration of minerals.

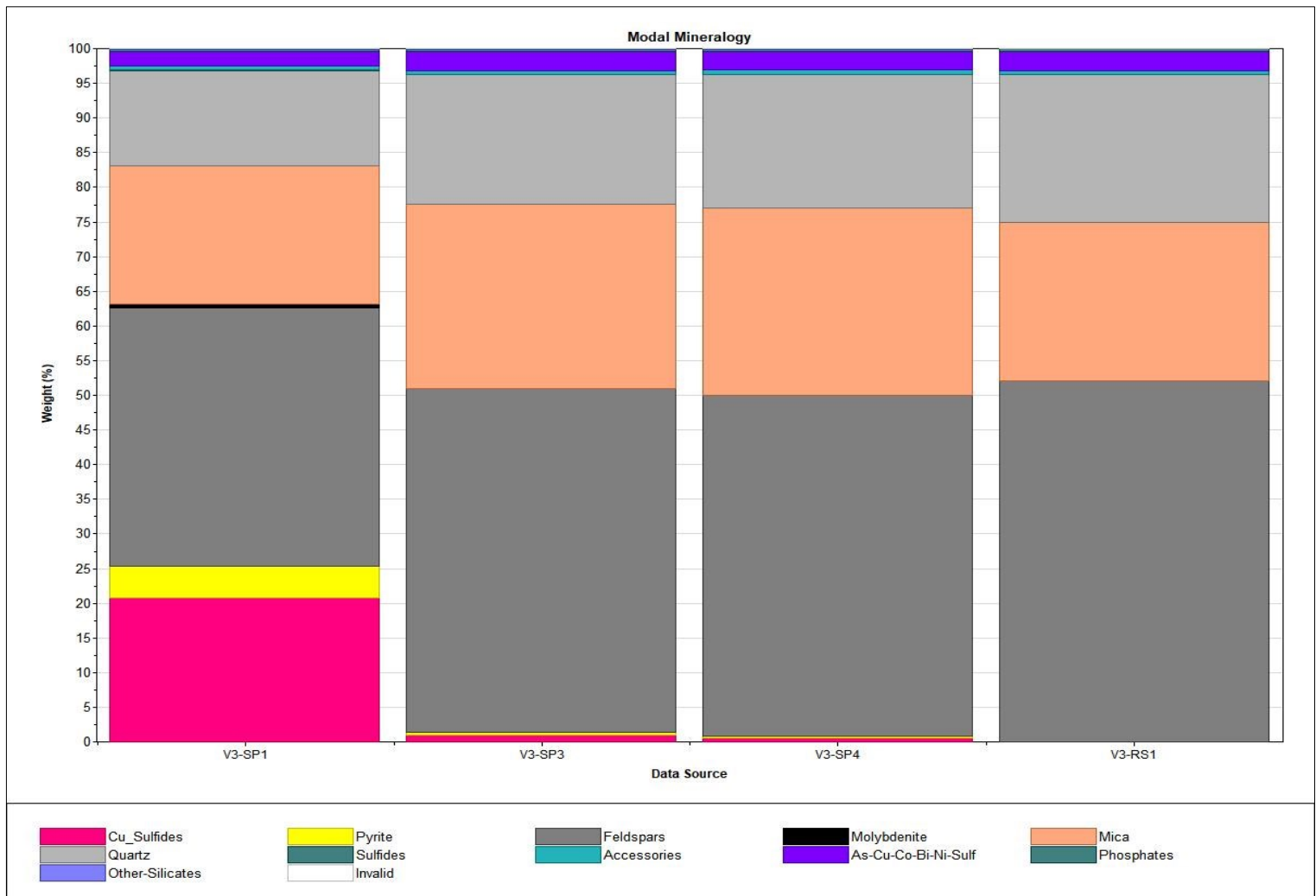


Figure 2. Modal Mineralogy of the concentrate (V3-SP1, SP3, SP4) and tailing (V3-RS1)

2. Description of the copper sulfide, the pyrite, and the molybdenite particles in concentrate and tailing

A detailed description of the various particles extracted from the porphyry copper samples, both from the concentrate and tailings, will be provided to gain deeper insights into these minerals. This analysis will focus on the minerals mentioned, including copper sulfides, pyrite, molybdenite. Figure 3 and Figure 4 shows the distribution of different minerals in both the concentrate and the tailing

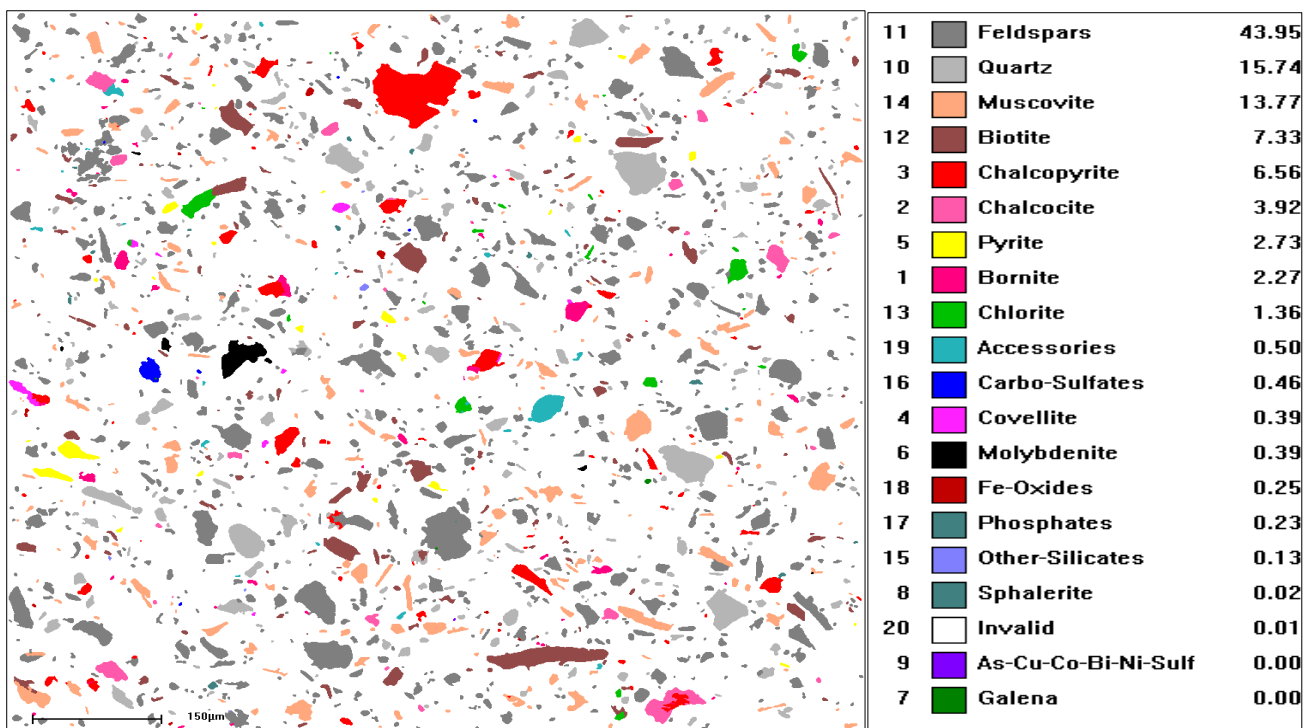


Figure 3. Minerals distribution in the Concentrate (V3-SPI) at a scale of 150 μm

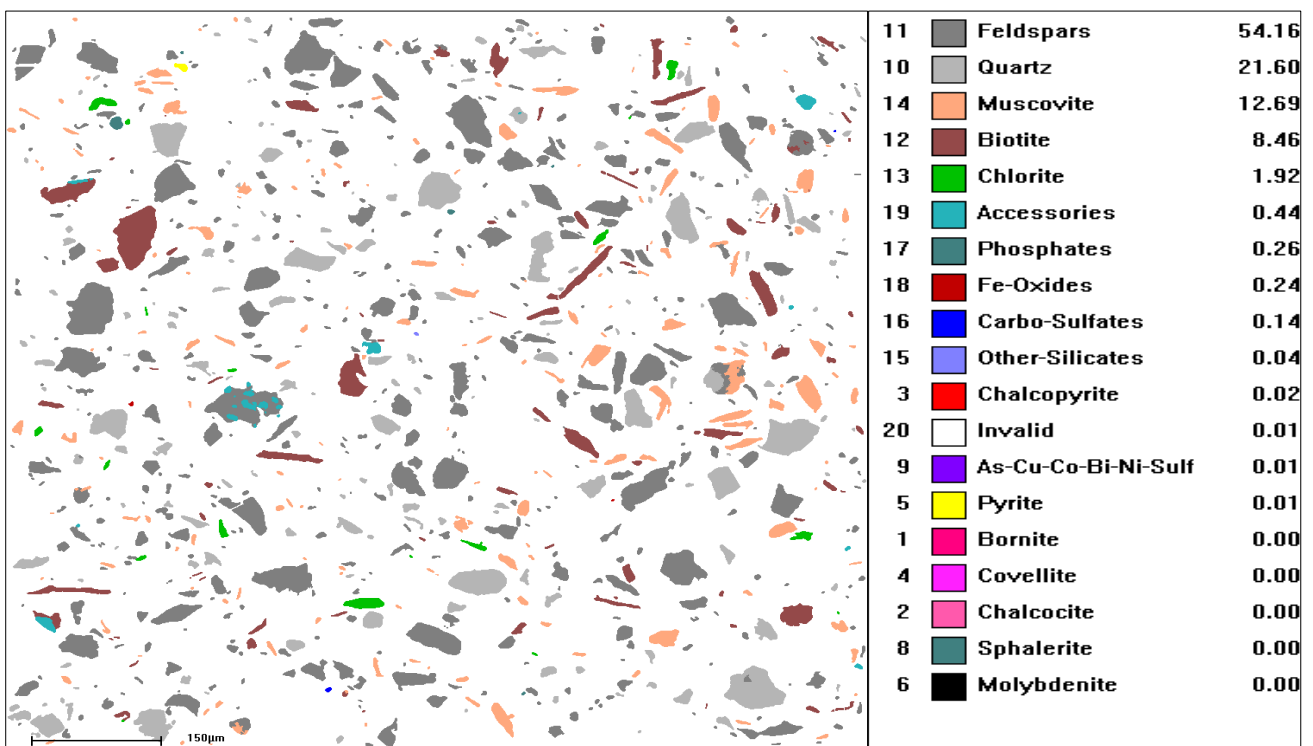


Figure 4. Minerals distribution in the tailing (V3-RS1) at a scale of 150 μm

2.1. Description of the different mineral particles

2.1.1. Chalcopyrite

A size range of 85-100 μm is observed in the concentrate V3-SP1, with grains appearing in quadratic, rectangular, and triangular shapes, as shown in Figure 5. Additionally, Chalcopyrite in the concentrate is often covered with Chalcocite and Bornite, as shown in Figure 6. Chalcopyrite, a primary copper mineral, can undergo chemical transformation under supergene conditions, where it reacts with acidic, oxygenated waters. This reaction often results in secondary copper minerals like Chalcocite and Bornite, which form a coating or mantle around the Chalcopyrite(Zhao et al. 2014). As shown in Figure 6, most of the Chalcopyrite grains in the tailing sample V3-RS1 are small, averaging around 10 μm in size, and showing similar shapes to those found in the concentrate

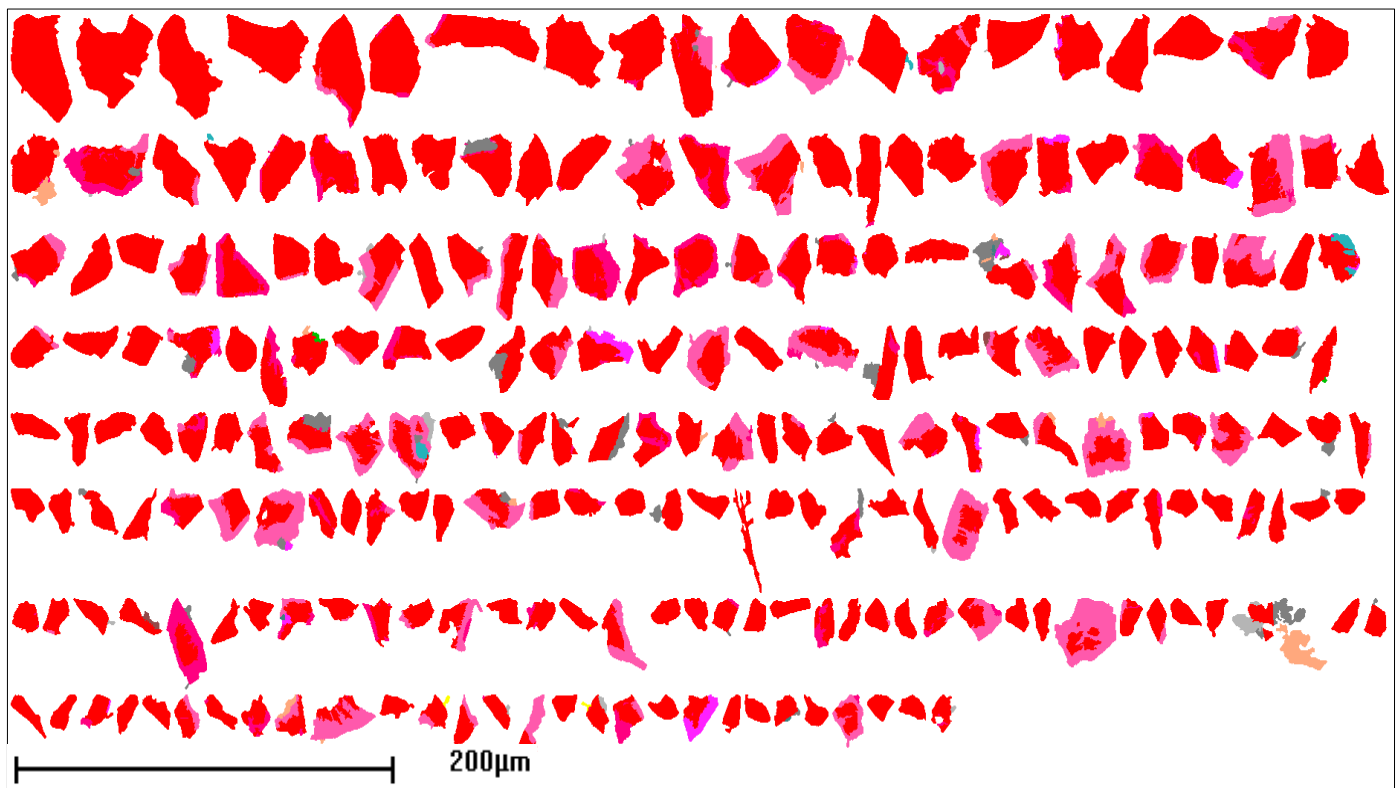


Figure 5. Chalcopyrite Particles in Concentrate V3-SP1 at scale of 200 μm

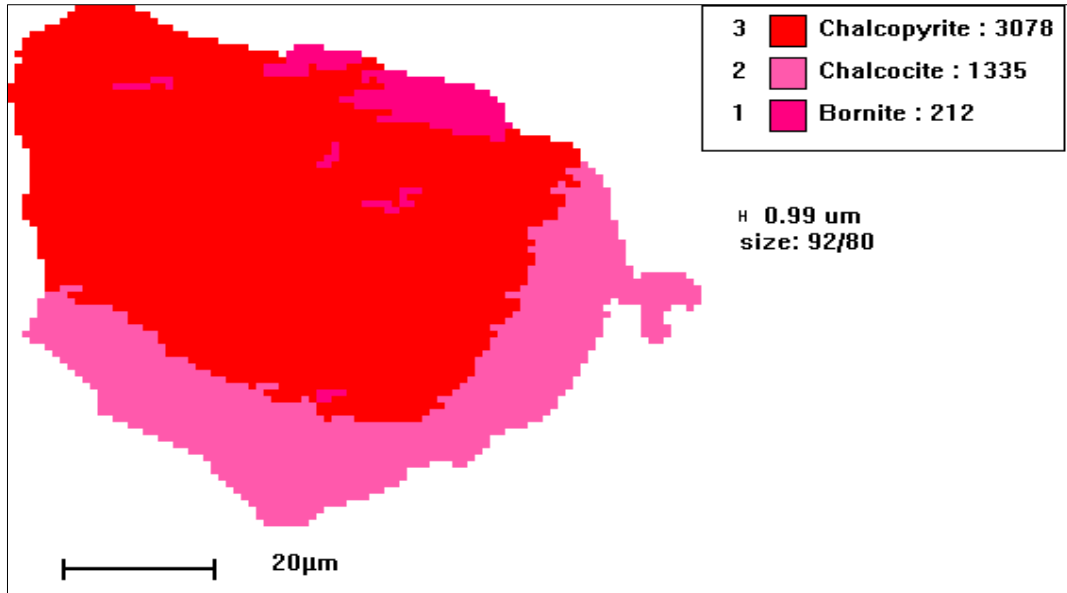


Figure 6. Chalcopyrite grain mantled with Chalcocite and Bornite in V3-SP1 at scale of $20\text{ }\mu\text{m}$

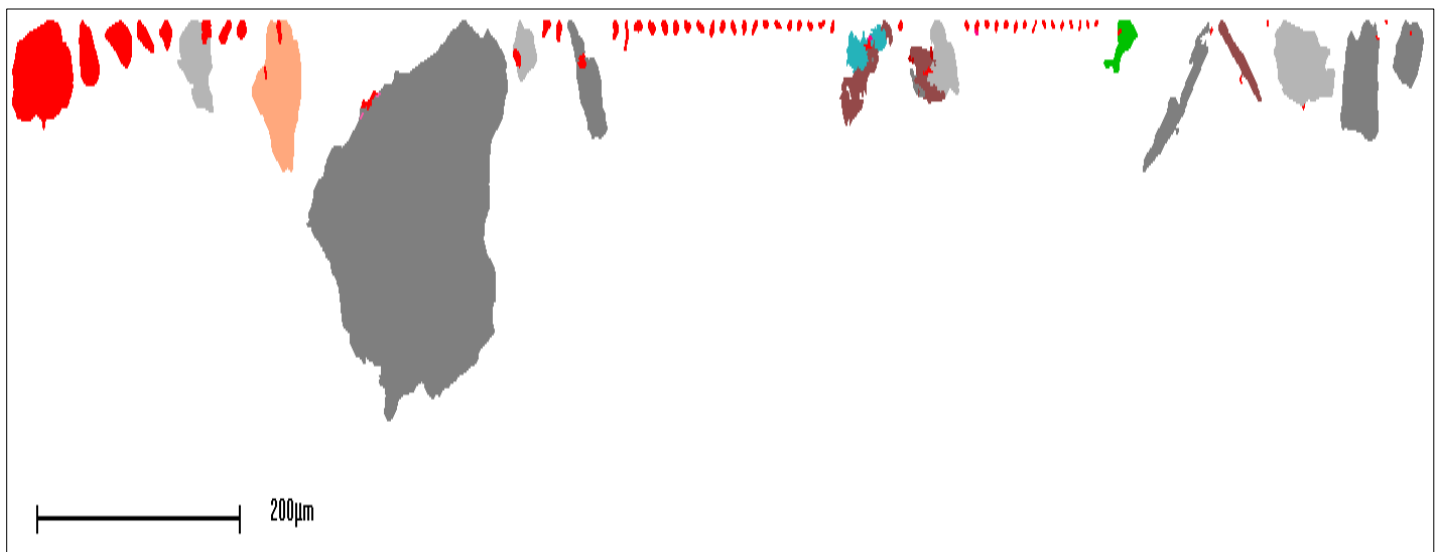


Figure 7. Chalcopyrite particles in tailing V3-RS1 at scale of $200\text{ }\mu\text{m}$

2.1.2. Pyrite

The V3-SP1 concentrate features grains with a size range of $70\text{-}100\text{ }\mu\text{m}$, showing a variety of irregular shapes such as quadratic, rectangular, flat, and triangular, as illustrated in Figure 8. Most of these grains have sharp edges, though some display sloped, curved, rough, or rounded edges. In addition, Figure 9 shows little amount of Pyrite in the tailing. Figure 10 reveals the presence of minerals including quartz, feldspars, muscovite, biotite, and chalcocite, alongside pyrite. These mineralogical components are often a result of the geological

formations and alteration processes that have taken place over time. Such minerals are typically found in porphyry copper deposits, where chalcopyrite is the main copper-bearing mineral as Zit was previously reported(Kavalieris et al. 2017).

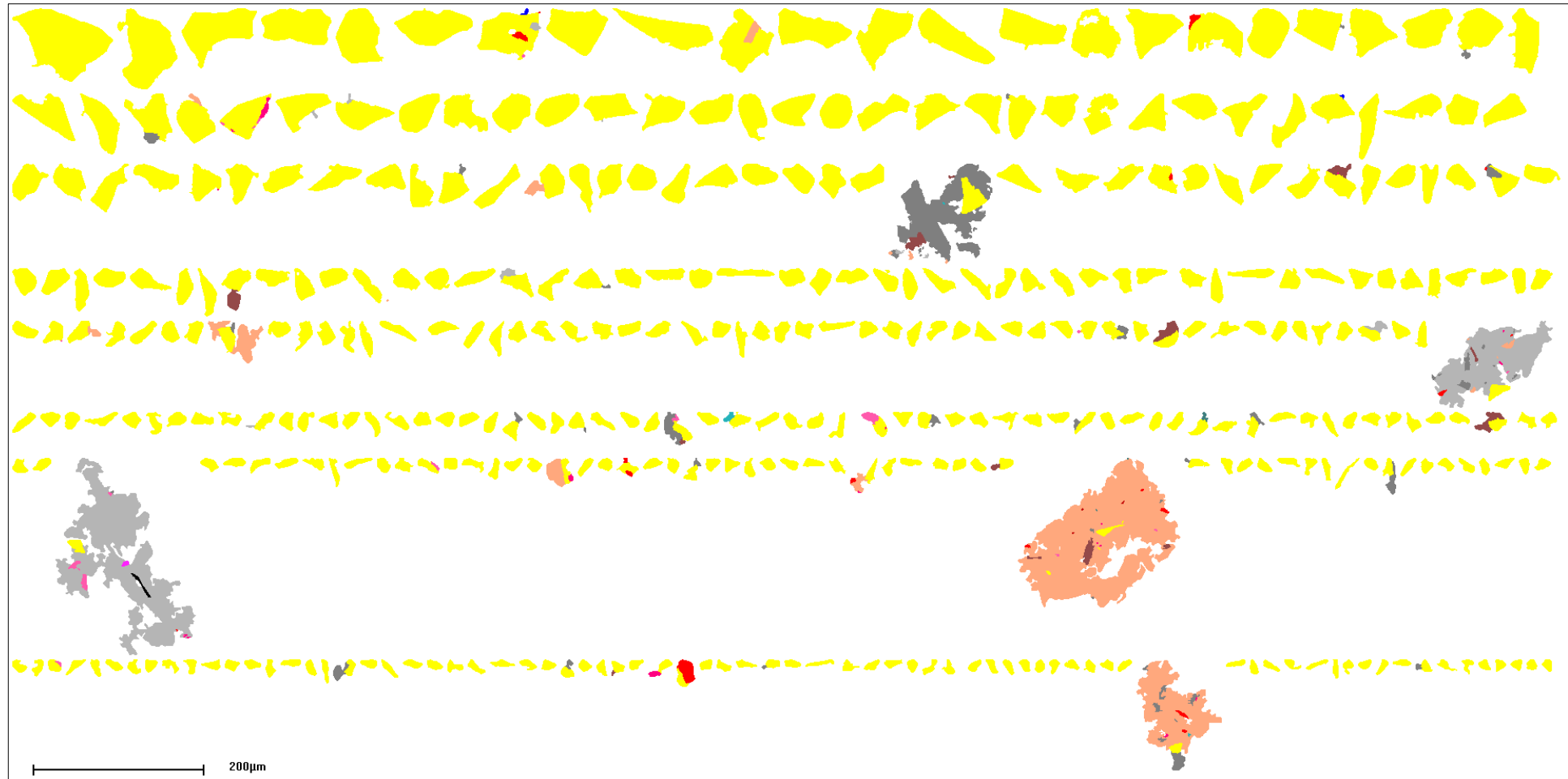


Figure 8. Pyrite particles in concentrate V3-SP1 at scale of 200 μm

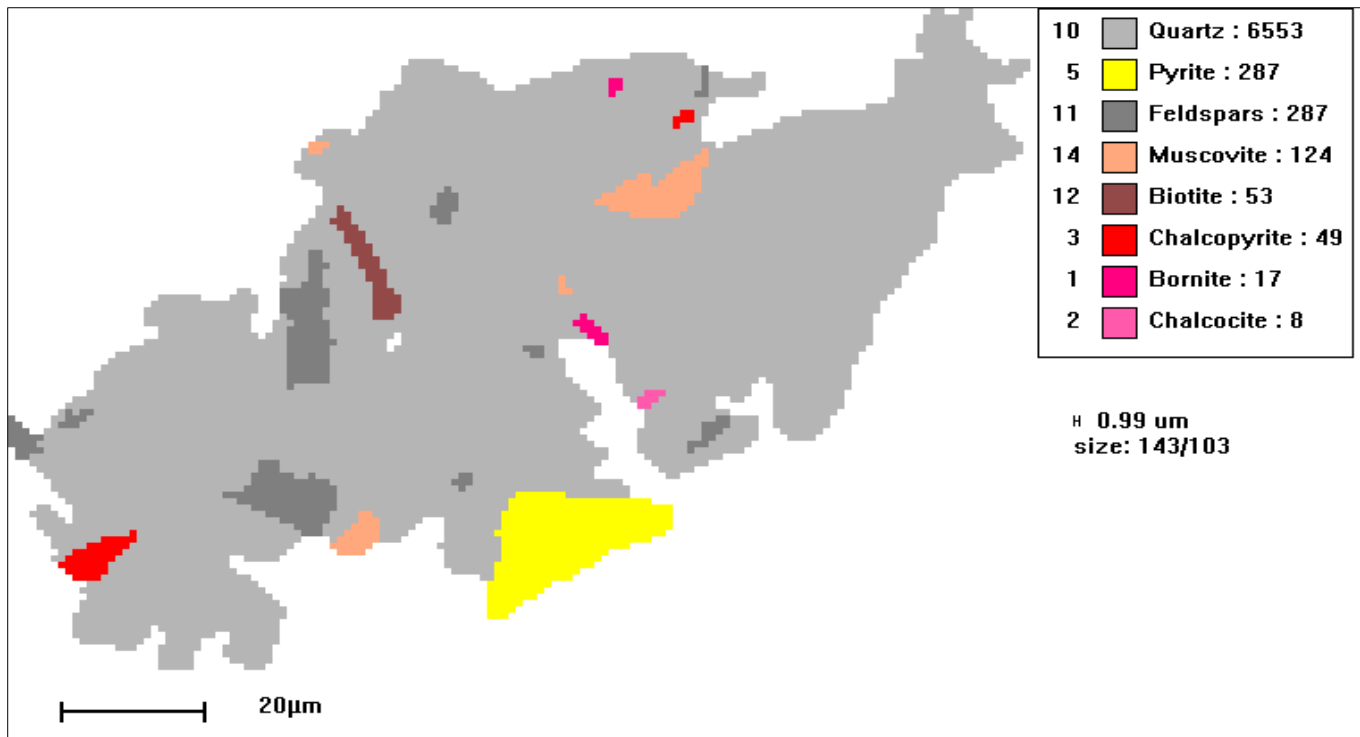


Figure 9. Pyrite particle mantled with some minerals mentioned in the legend in V3-SP1 at a scale of 20 μm



Figure 10. Pyrite particle distribution in tailing V3-RS1 at a scale of 100 μm

2.1.3. Molybdenite

Figure 11 illustrates that most of the molybdenite in the concentrate is nearly rectangular and flat, with the presence of smaller grains and a few of average size. The edges of these grains vary, with some being sharp, others rounded, and a few showing sloped, curved, or rough characteristics.

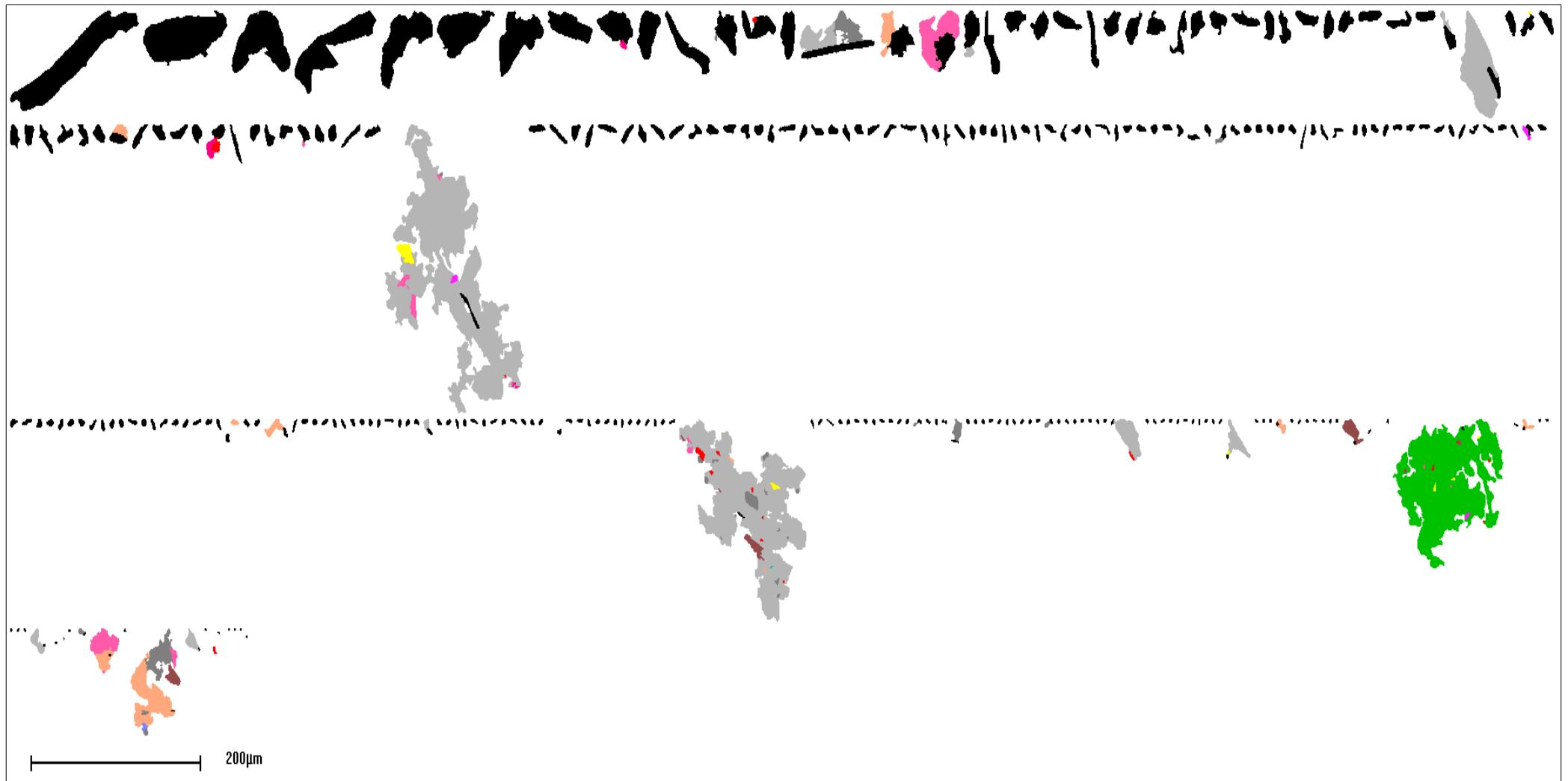


Figure 11. Molybdenite particles distribution in tailing V3-RS1 at a scale of 200 μm

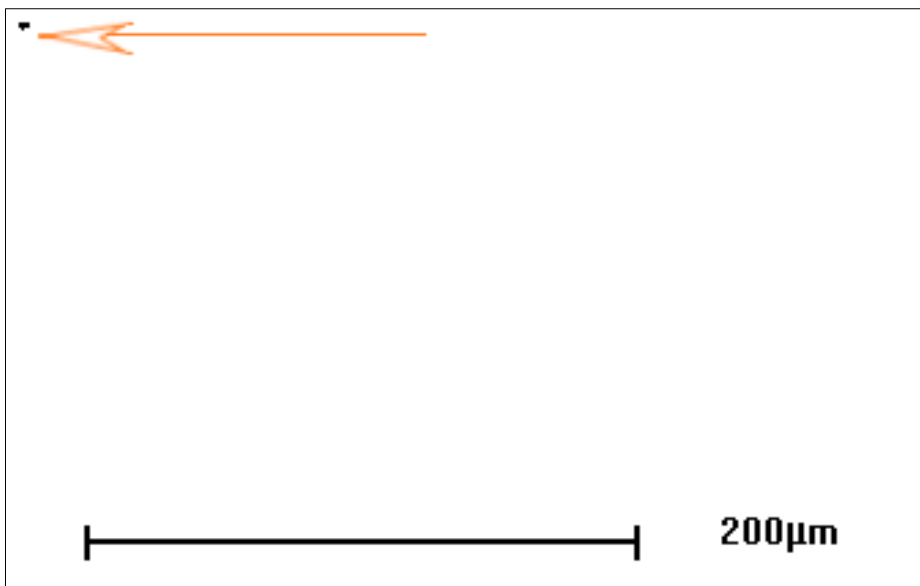


Figure 12. Molybdenite particles distribution in tailing V3-RS1 at a scale of 200 μm

2.1.4. Bornite

The bornite grains in the concentrate have a size of 100 μm , showing a variety of irregular shapes, including polygons, quadratics, rectangles, and triangles, as shown in Figure 13. The edges of these grains are primarily sharp or rounded, with some being sloped, curved, or rough. In contrast, the bornite grains in the tailings sample V3-RS1 are much smaller, around 5 μm in size, with a relatively low amount of bornite, as illustrated in Figure 14. Figure 15 shows an example of a bornite grain in the concentrate (V3-SP1) surrounded by quartz, a feature characteristic of hydrothermal environments, particularly in porphyry copper deposits. Bornite, a copper iron sulfide, forms from copper-rich fluids at high temperatures, while quartz, a common mineral, precipitates from silica-rich fluids as they cool. Their close association is due to the similar conditions under which they form in these geological settings(Hermo et al. 2022).

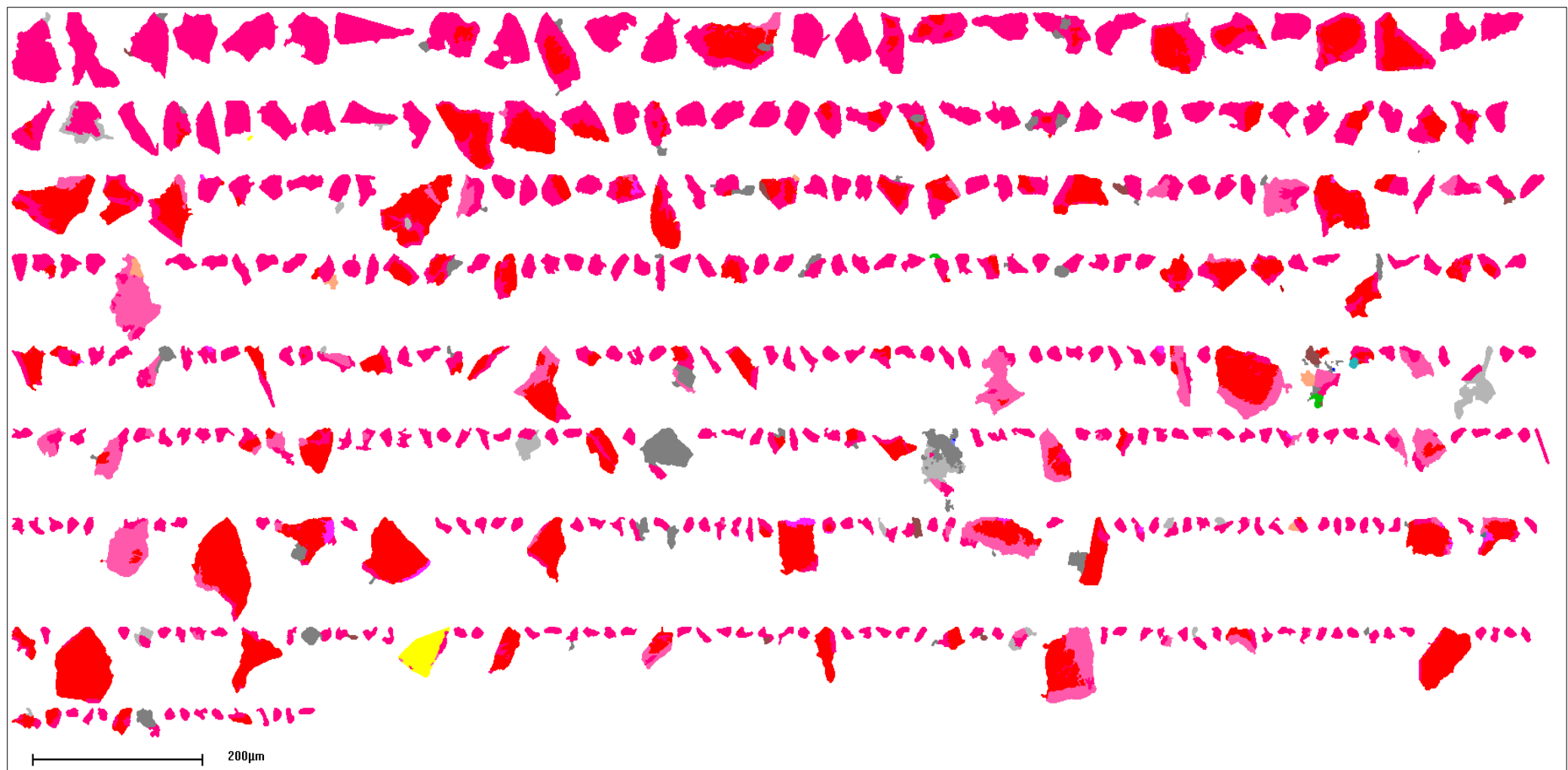


Figure 13. Bornite particles distribution in concentrate V3-SPI at a scale of $200 \mu\text{m}$

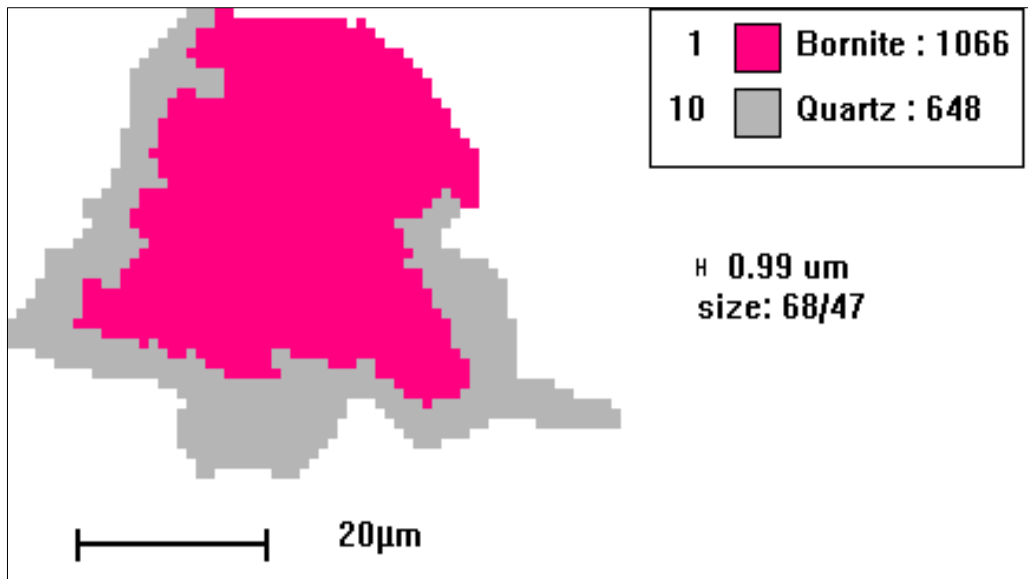


Figure 14. Bornite particle mantled with quartz in concentrate V3-SP1 at a scale of 20 μm



Figure 15. Bornite particles distribution in tailing V3-RS1 at a scale of 200 μm

2.1.5. Chalcocite

The chalcocite grains in the concentrate (V3-SP1) displays various irregular shapes, including rectangular, quadratic, and triangular forms, with an average grain size of approximately 100 μm as illustrated in Figure 16. In contrast, the chalcocite grains in the tailings (V3-RS1) are predominantly rounded, with a few having sharp edges. These grains are much smaller, around 5 μm in size, and the overall amount of chalcocite in the tailings is minimal, as shown in Figure 17. In addition, As shown in Figure 18, it can be seen that Chalcopyrite and chalcocite often occur together, which could be related to the hydrothermal processes and secondary enrichment. Chalcopyrite forms as a primary copper-iron sulfide mineral in high-temperature hydrothermal systems, while chalcocite typically forms later

through secondary enrichment, where chalcopyrite is altered by groundwater, increasing the copper content. This process is common in porphyry copper deposits as stated by (Chen, Peng, and Bradshaw 2014).

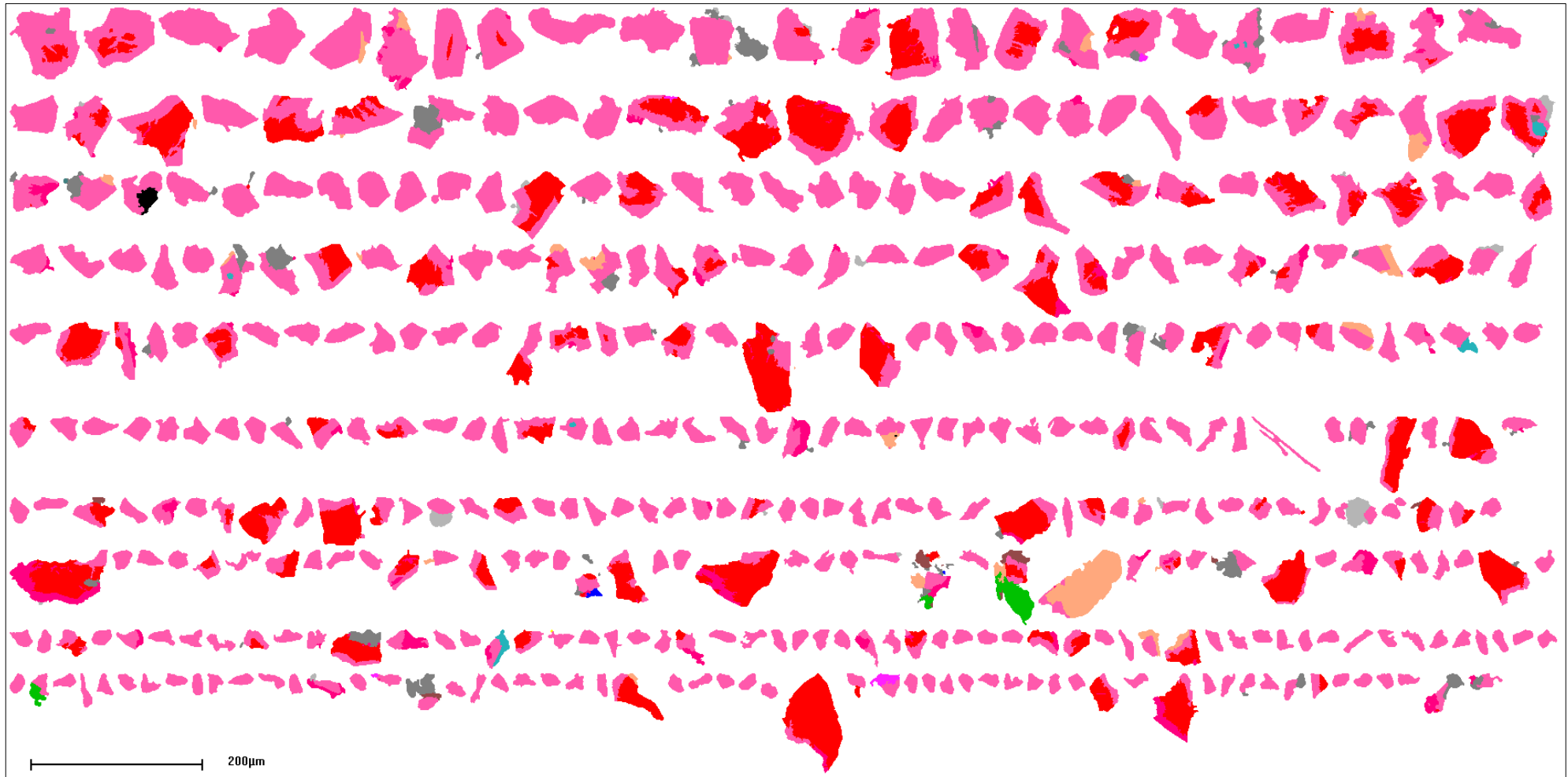


Figure 16. Chalcocite particles distribution in concentrate V3-SPI at a scale of 200 μm

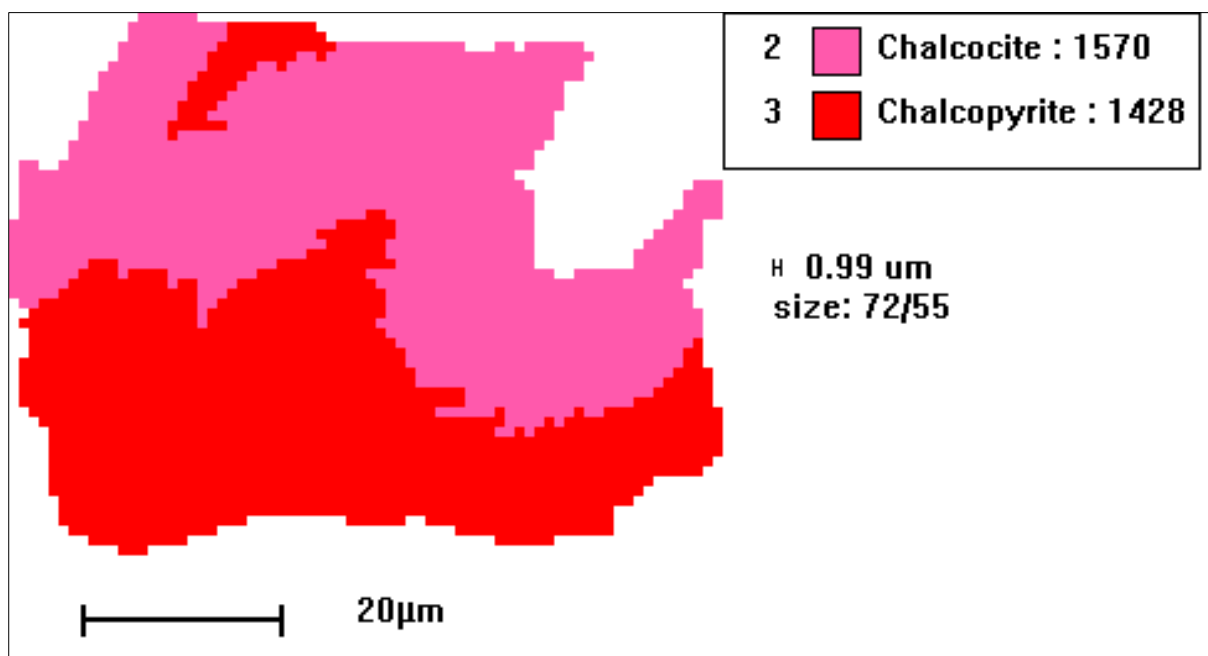


Figure 17. Chalcocite particle occurring with Chalcopyrite particle in concentrate V3-SP1 at scale of 20 μm

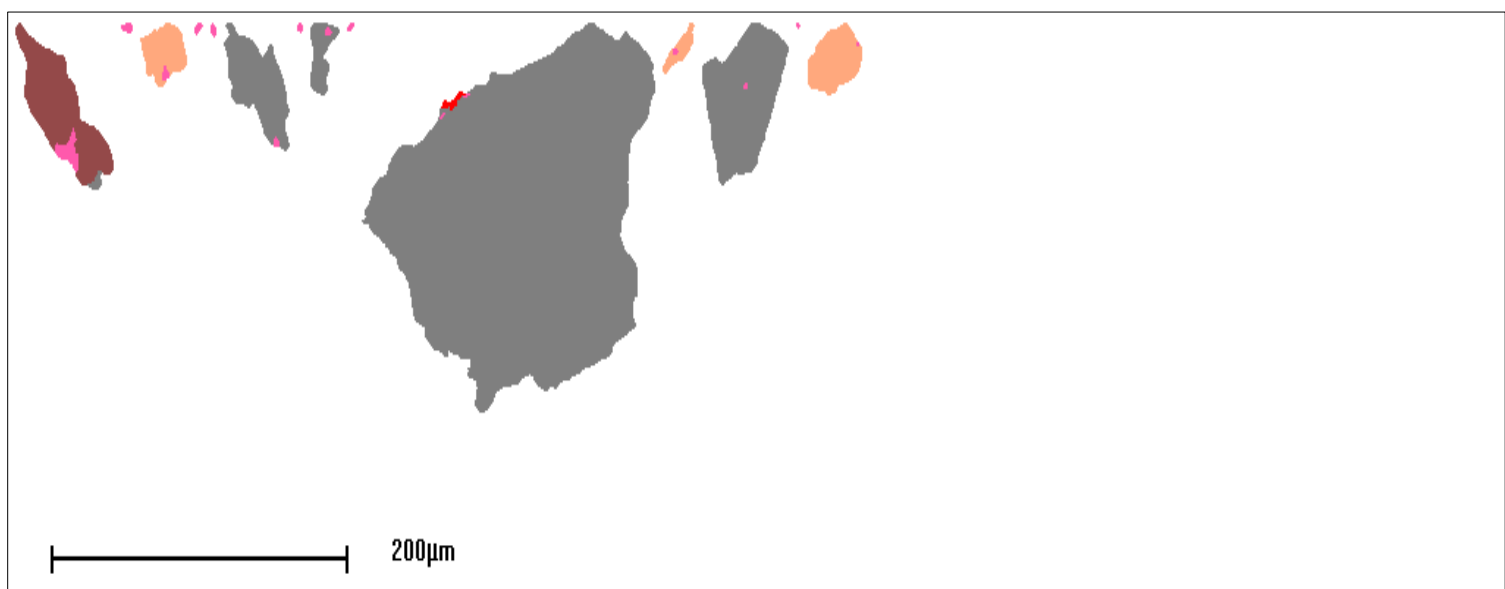


Figure 18. Chalcocite particles occurring in tailing V3-RS1 at a scale of 200 μm

2.1.6. Covellite

Covellite grains in the concentrate V3-SP1 shows various irregular shapes, such as rectangular, quadratic, and triangular shapes, with a grain size of as shown in Figure 19. Additionally, in Figure 20, it can be seen the occurrence of Covellite with Chalcopyrite and Bornite and this is due to hydrothermal processes. According to (Sillitoe 2010) Covellite

typically forms through the weathering and alteration of chalcopyrite and bornite, especially in the near-surface supergene enrichment zone, where oxidation and lower temperatures promote its formation.

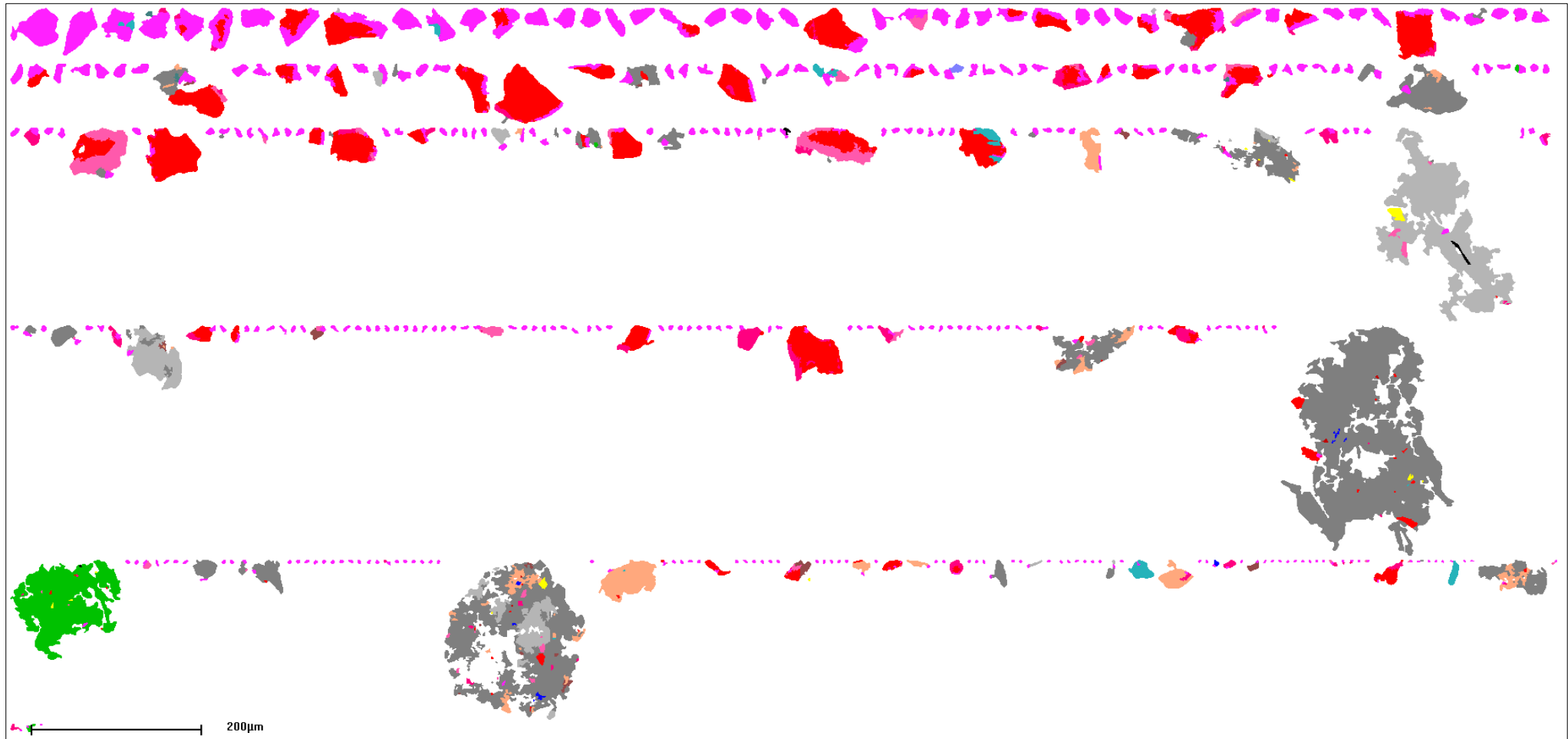


Figure 19. Covellite particles distribution in concentrate V3-SP1 at a scale of 200 μm

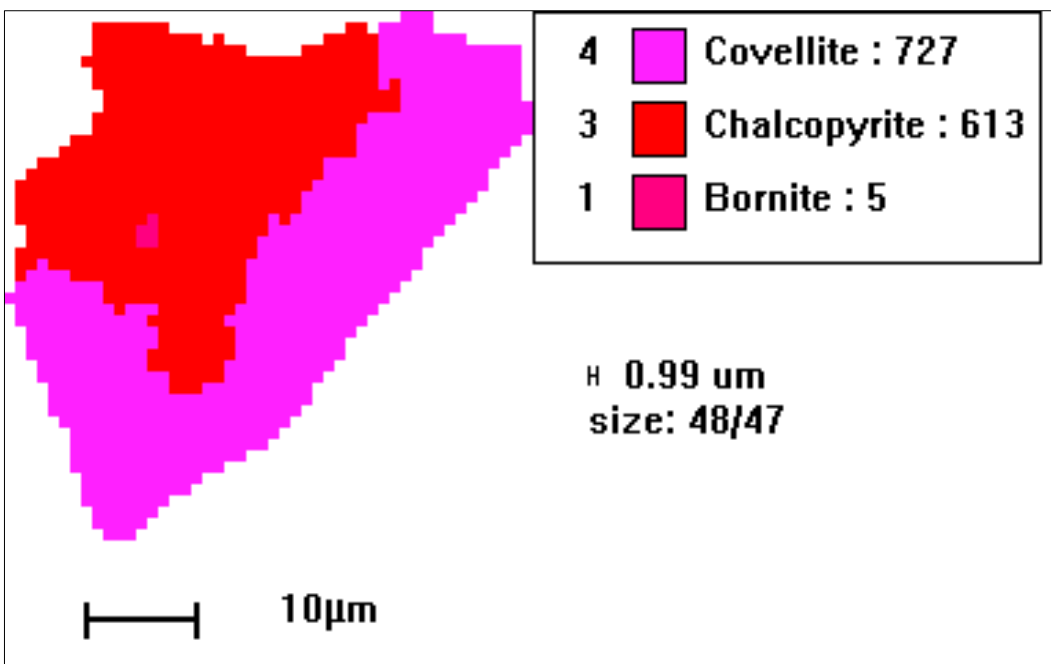


Figure 20. Covellite particle occurring with Chalcopyrite and Bornite particles in concentrate V3-SP1 at a scale of 10 μm

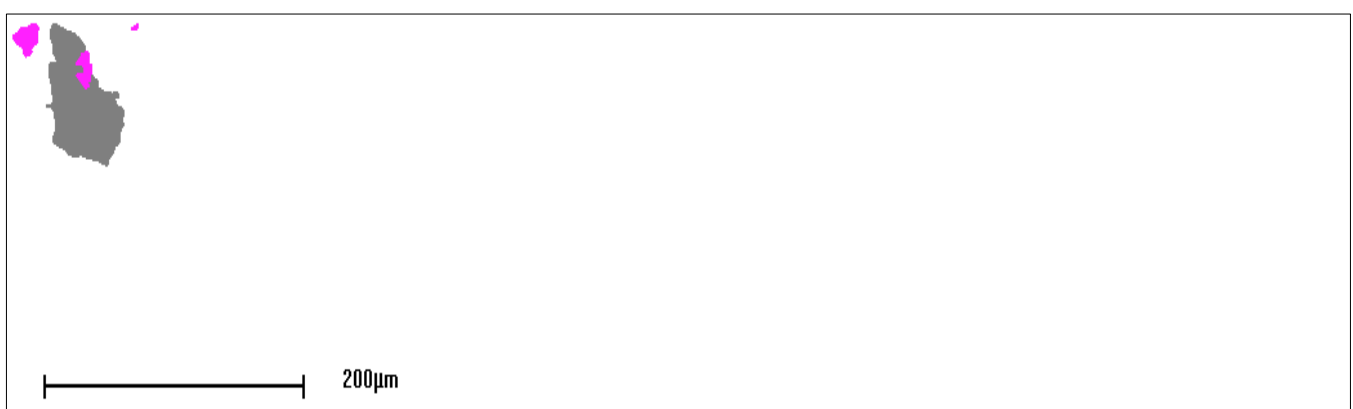


Figure 21. Covellite particles occurring in the tailing V3-RS1 at a scale of 200 μm

3. Preparing a shorter and convenient grouping list with copper minerals grouped together in the *mla database

Figure 22 shows the grouping list with copper minerals.

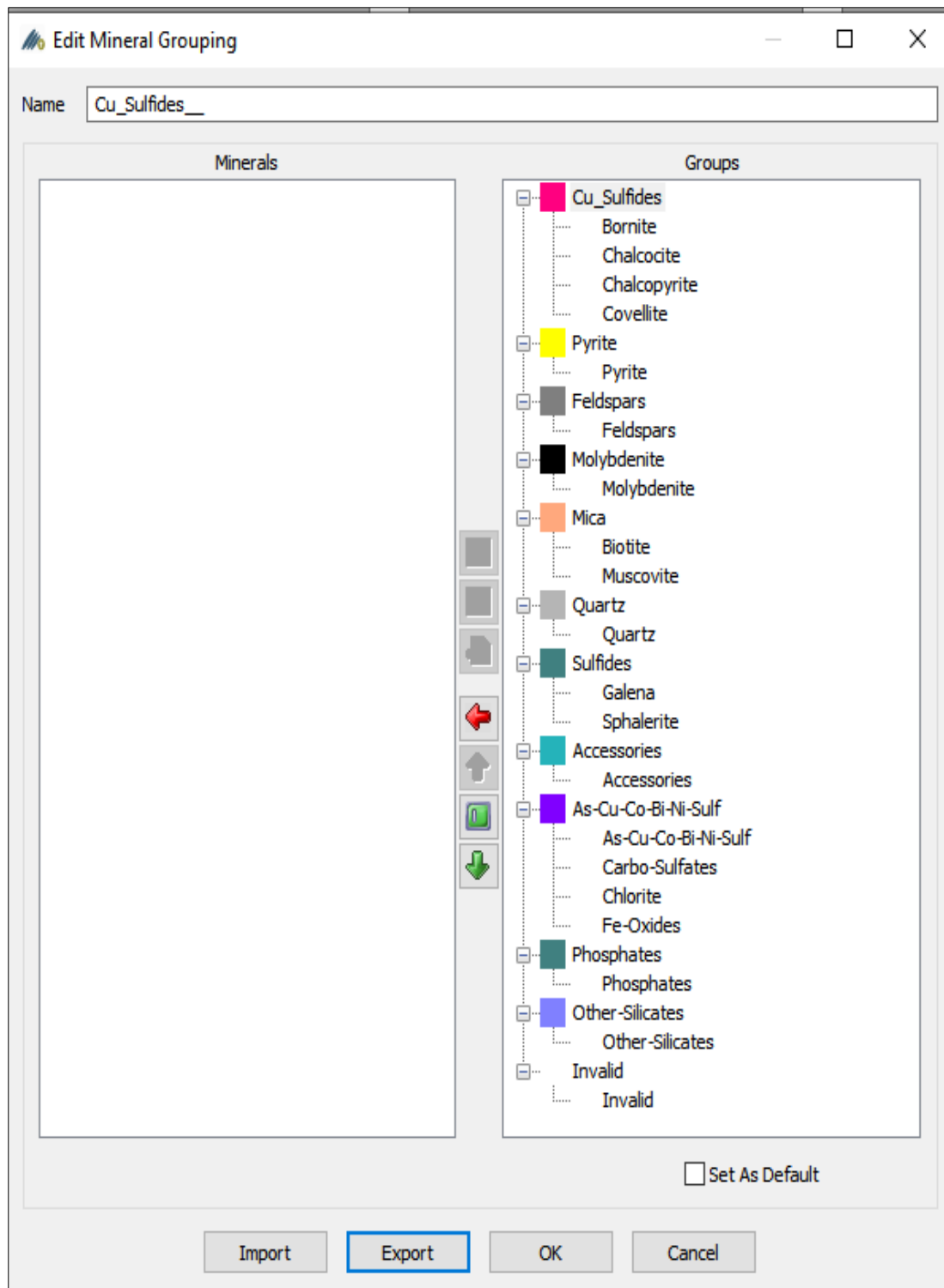


Figure 22. Minerals grouped by type

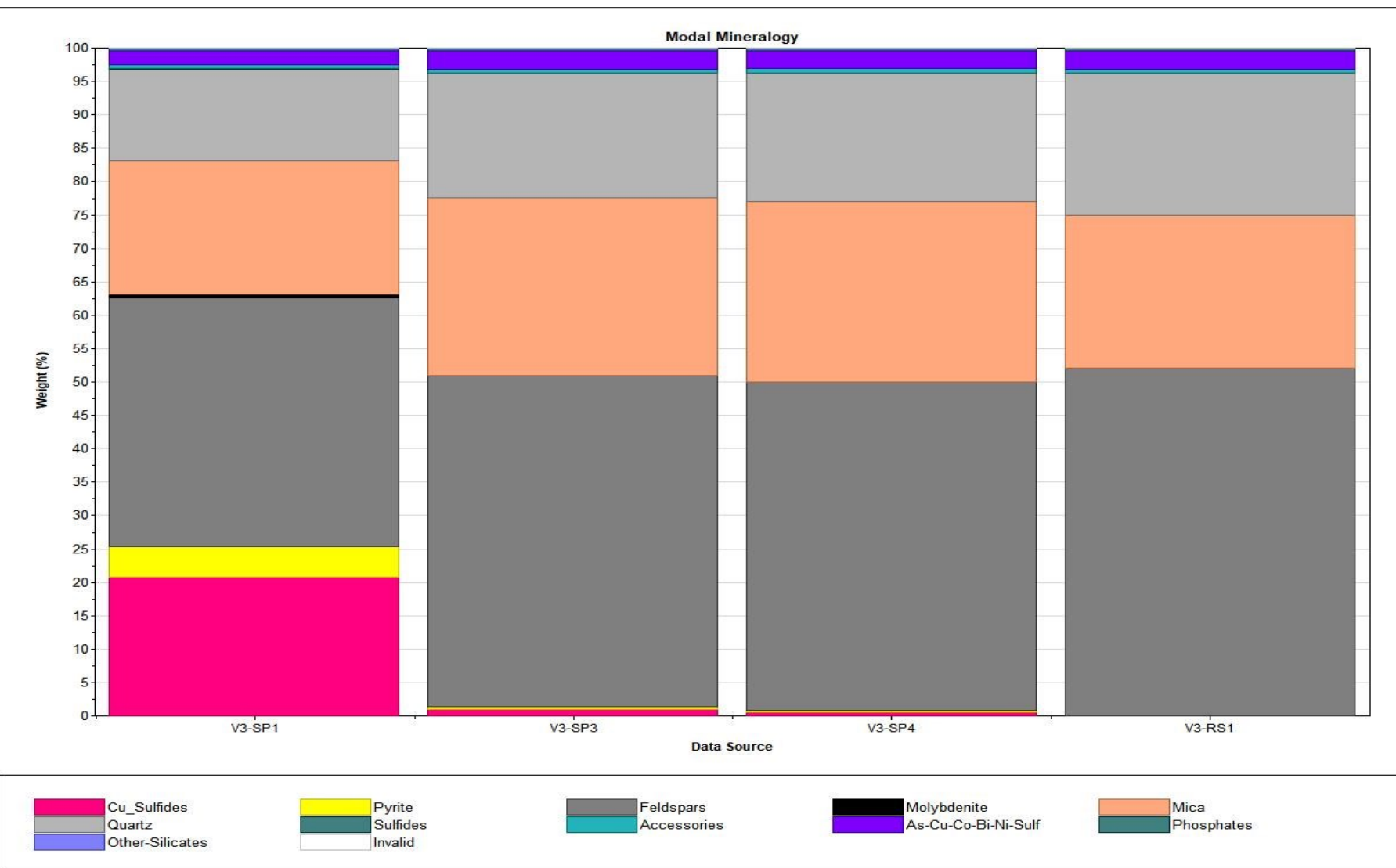


Figure 23. grouping of minerals, highlighting the grouping of copper-bearing minerals within the different concentrates (V3-SP1, SP3, SP4) and the tailing (V3-RS1) in MLA DataView

4. Preparing diagrams with the cumulative grain size distribution curves for copper minerals (grouped together), pyrite, quartz, feldspar, and mica from concentrate and the tailing with the lowest content of copper minerals

4.1. Grain size distribution curve for copper minerals in both the concentration (V3-SP1) and the tailing (V3-RS1)

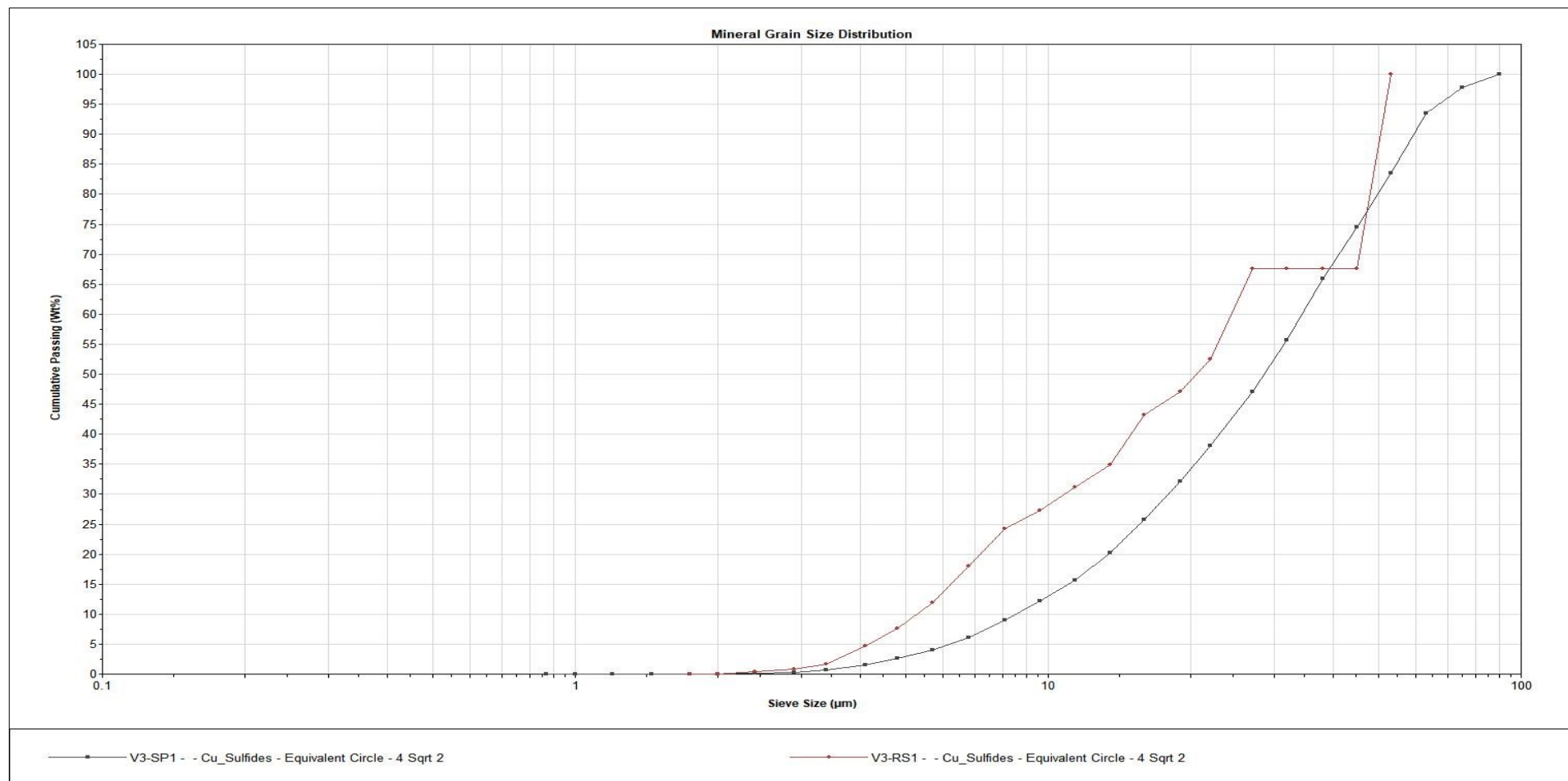


Figure 24. Copper minerals grain size distribution cure for the concentrate (V3-SP1) and the tailing (V3-RS1)

The grain size distribution curve for copper minerals in Figure 24 shows a very limited presence of Cu_Sulfides in the tailings, indicating that the largest grains are absent from the tailings. This suggests that the coarse particles are retained in the earlier processing stages.

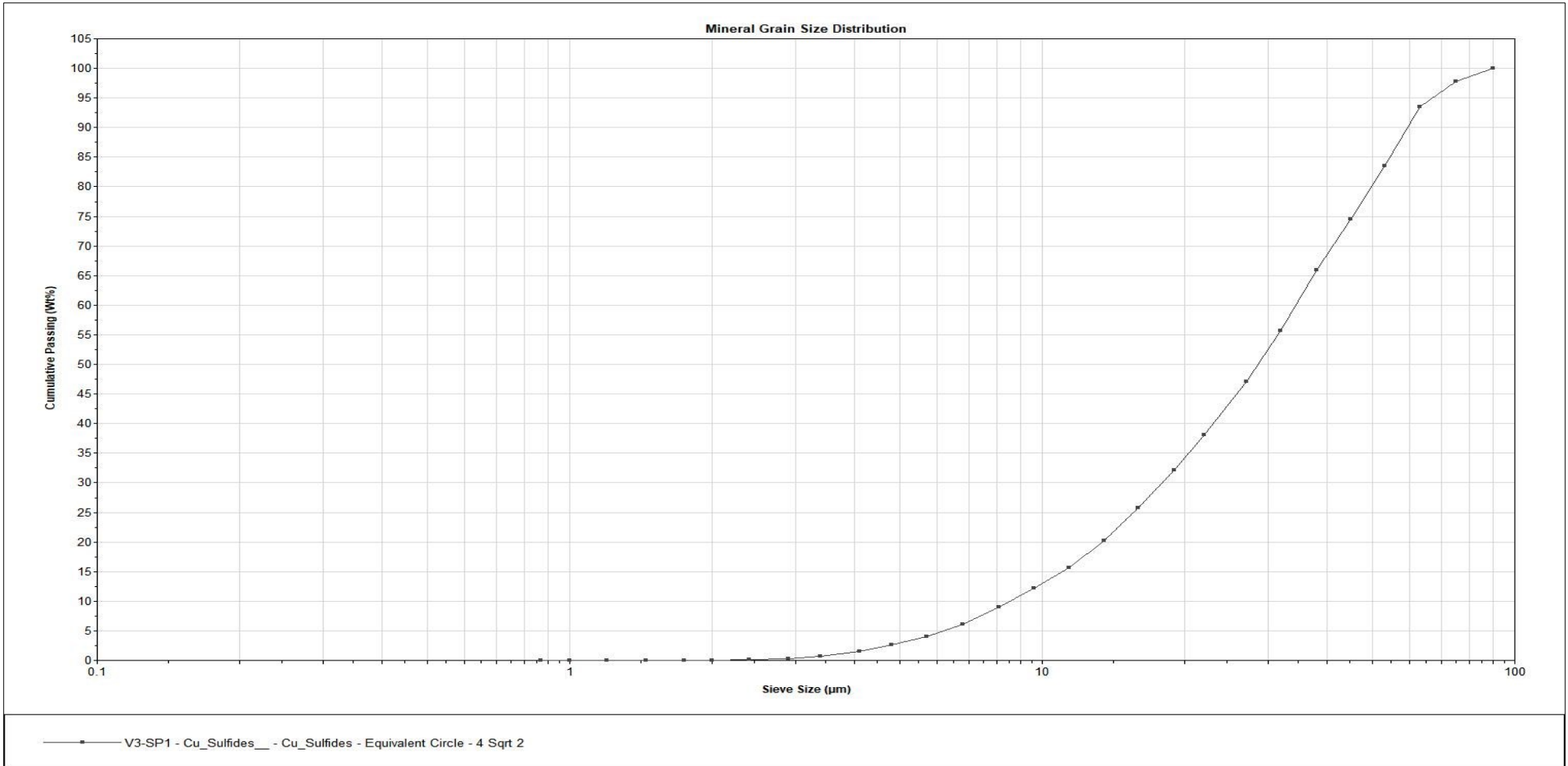


Figure 25. Grain size distribution curve for copper minerals in the concentrate (V3-SP1)

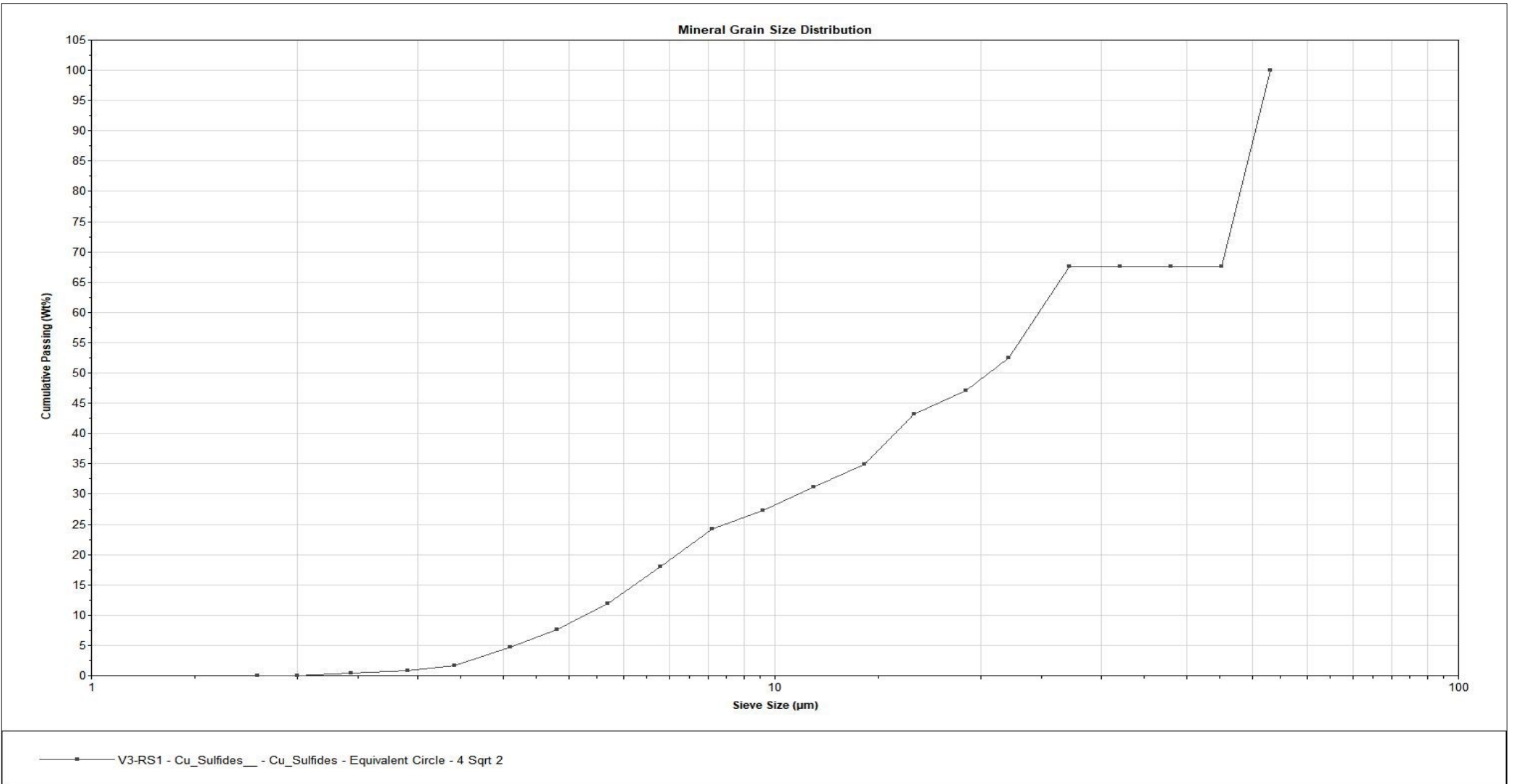


Figure 26. Grain size distribution curve for copper minerals in the tailing (V3-RS1)

4.2. Grain Size distribution curve for pyrite in both the concentrate (V3-SP1) and the tailing (V3-RS1)

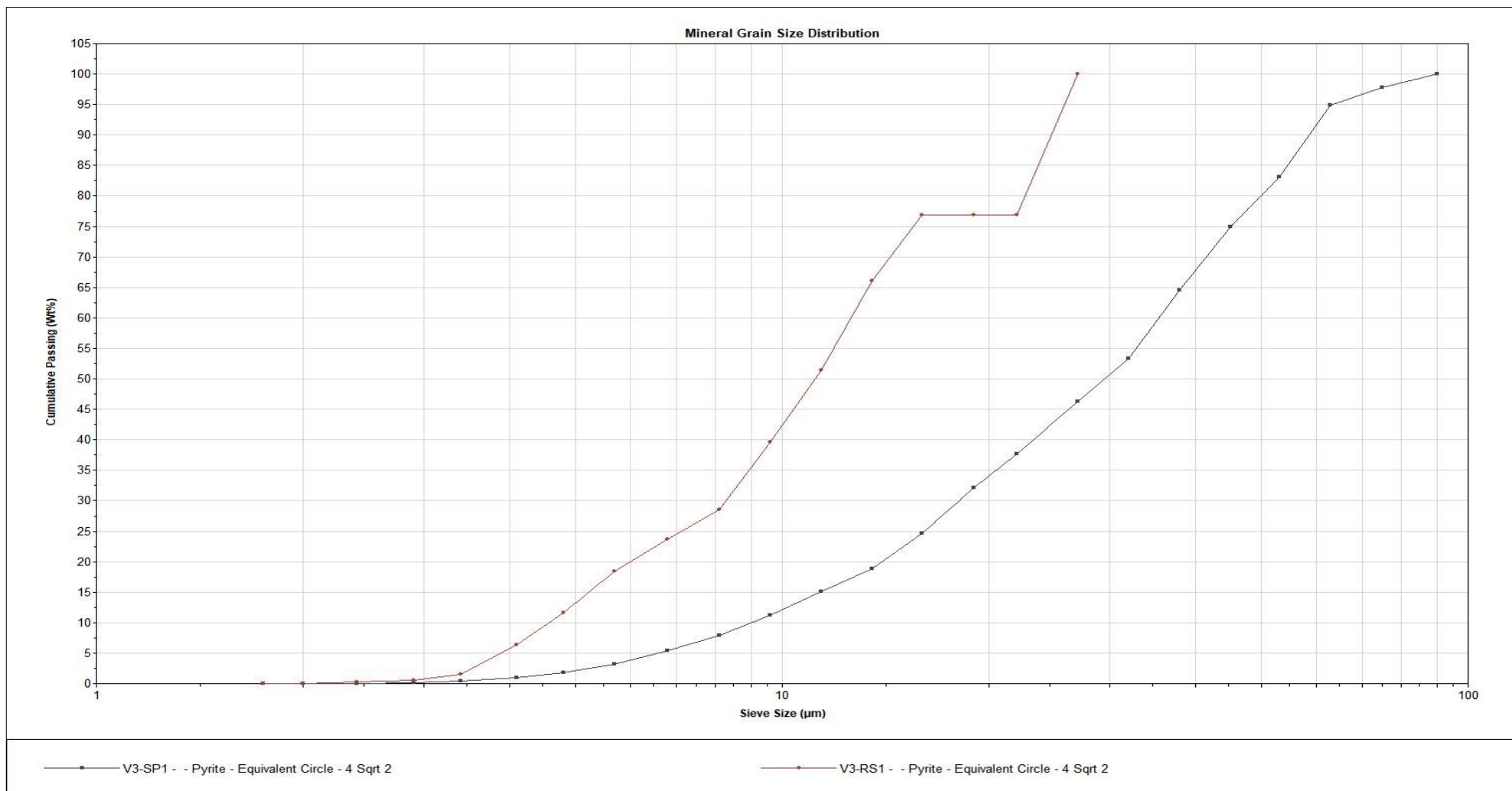


Figure 27. Grain size distribution curve for pyrite in the concentrate (V3-SP1) and the tailing (V3-RS1)

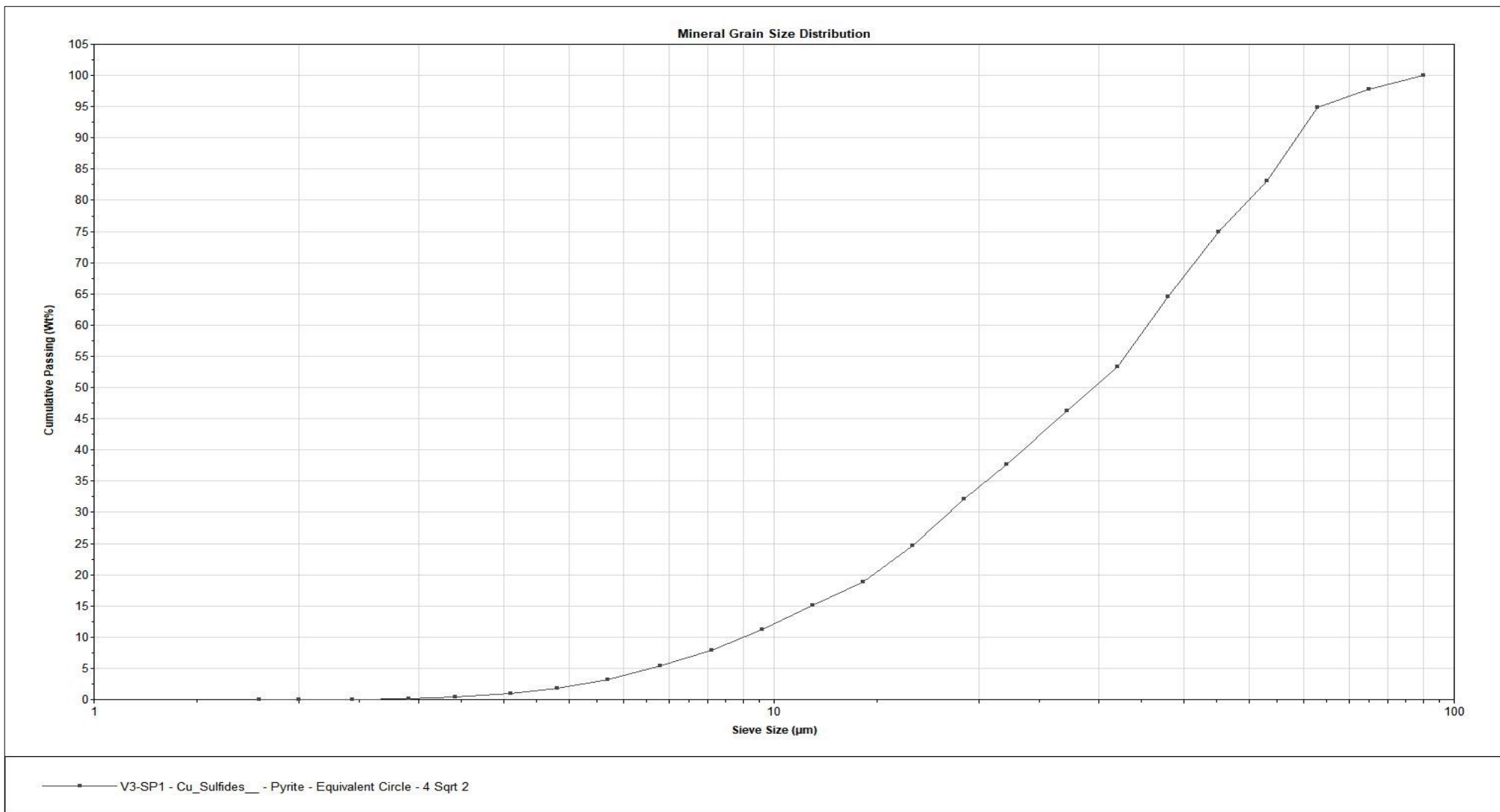


Figure 28. Grain size distribution curve for pyrite in the concentrate (V3-SP1)

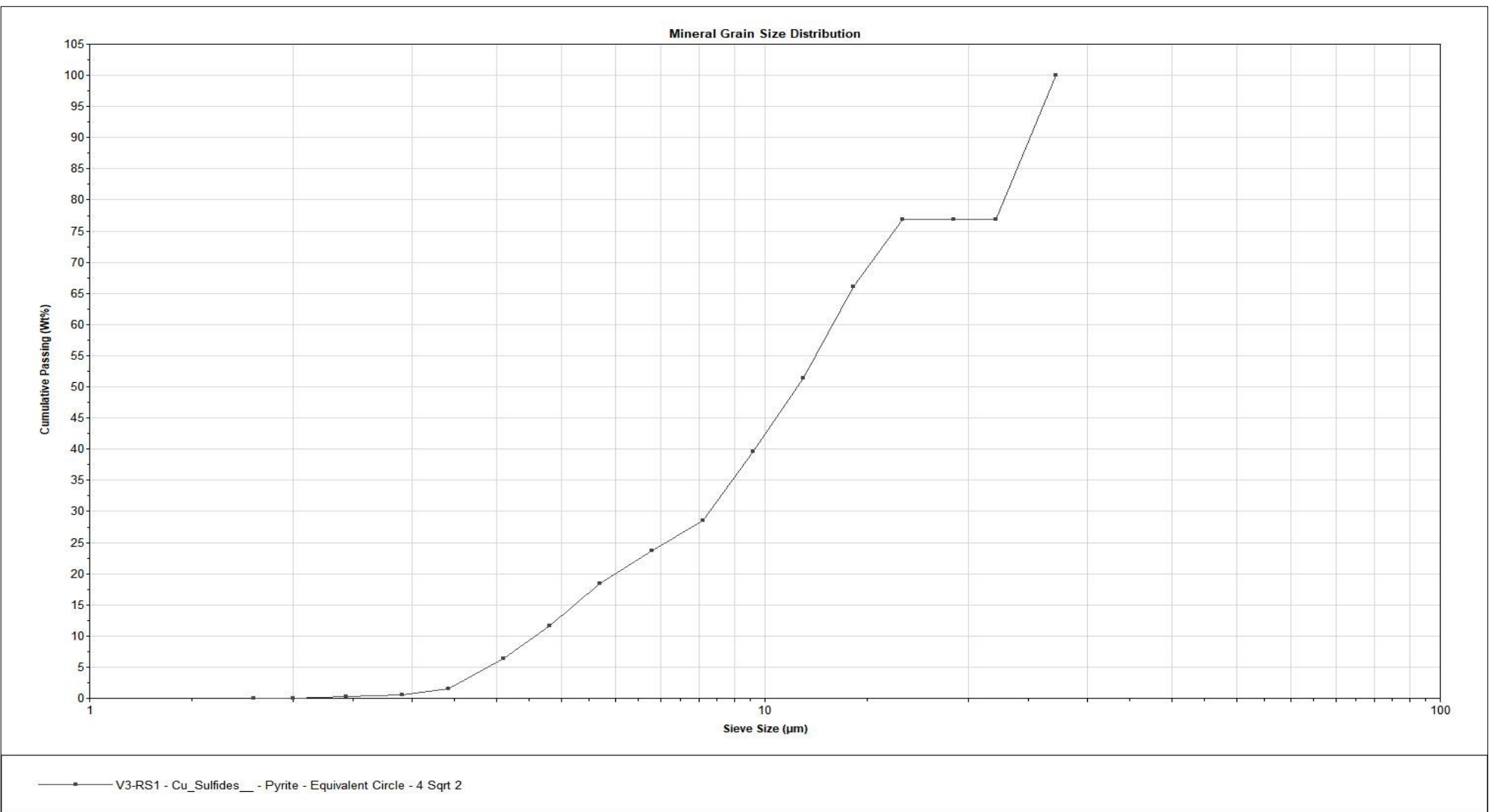


Figure 29. Grain size distribution curve for pyrite in the tailing (V3-RS1)

4.3. Grain size distribution curve for Quartz in both the concentrate (V3-SP1) and tailing (V3-RS1)

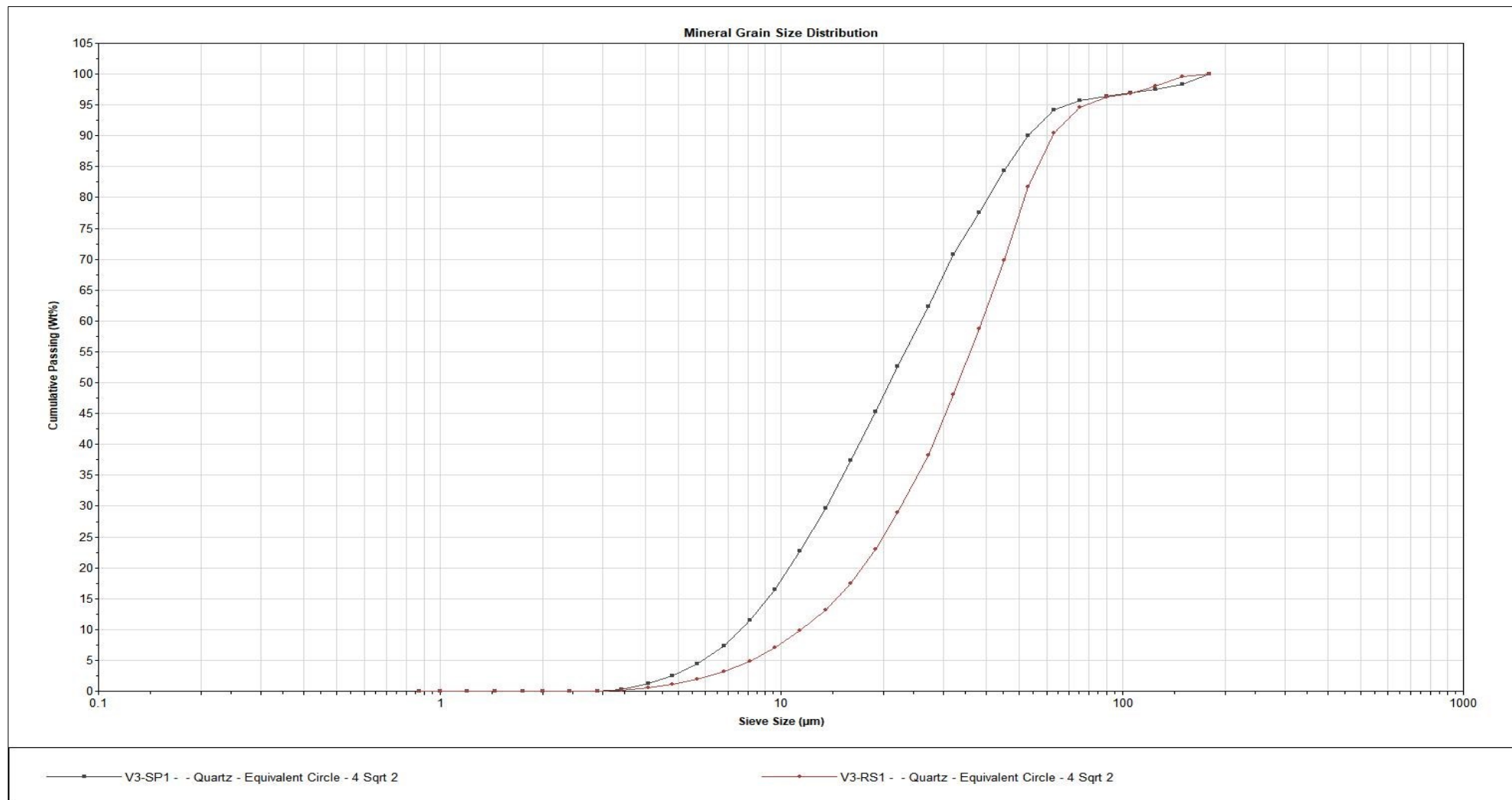


Figure 30. Grain size distribution curve for quartz in both the concentrate V3-SP1 and the tailing (V3-RS1)

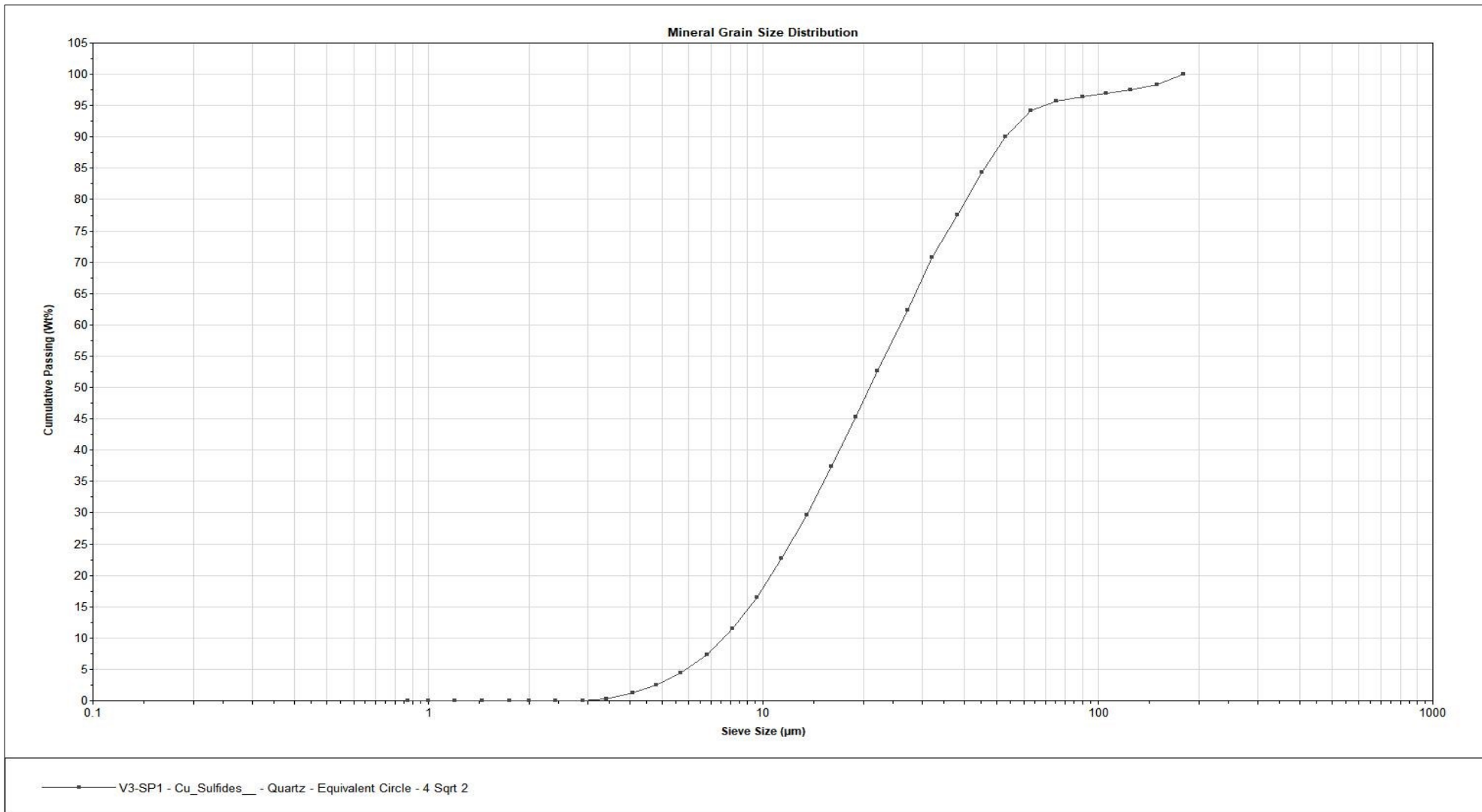


Figure 31. Grain size distribution curve for quartz in the concentrate (V3-SP1)

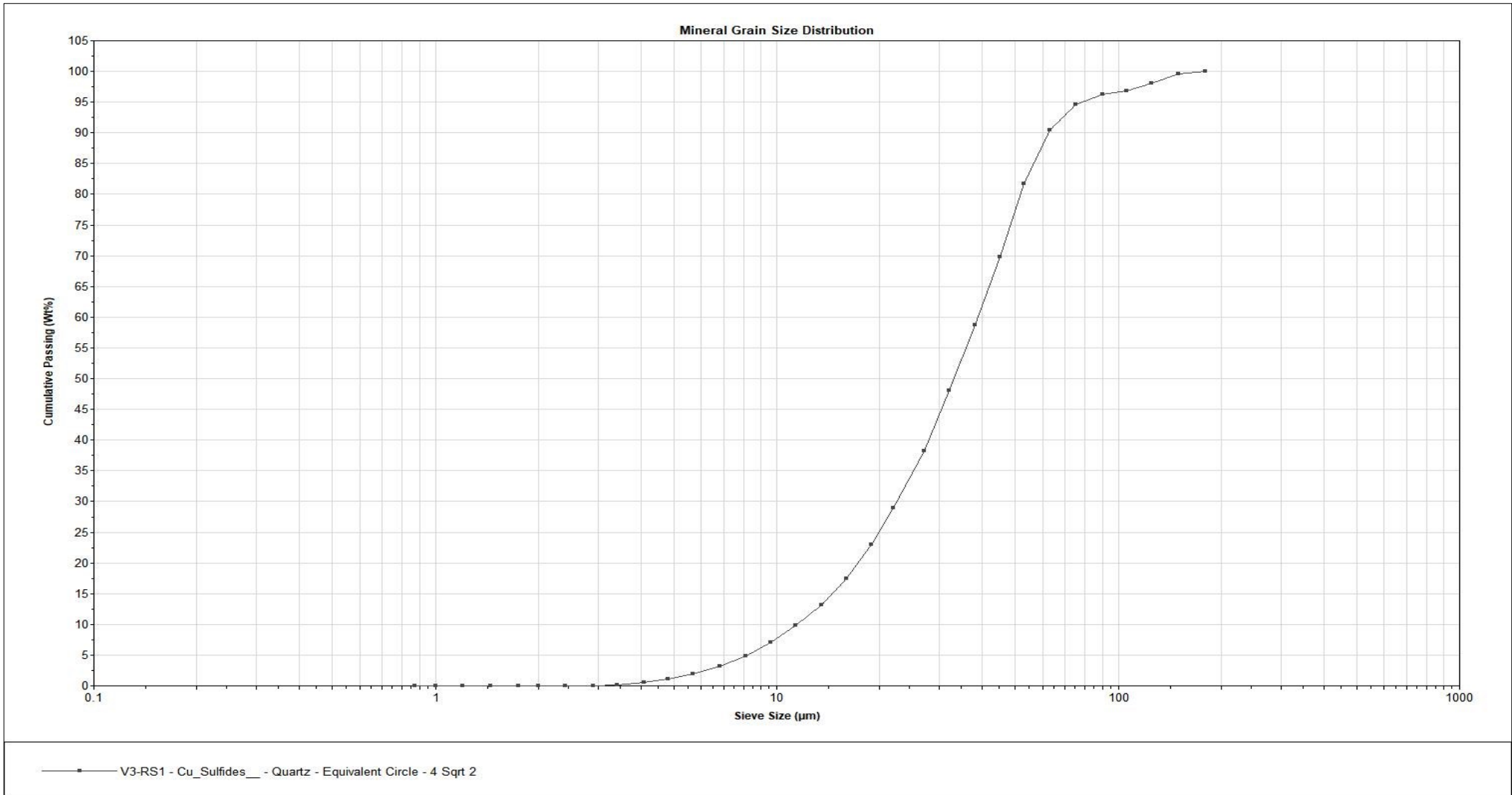


Figure 32. Grain size distribution curve for quartz in the tailing (V3-RS1)

4.4. Grain distribution curve for feldspar in the concentrate (V3-SP1) and the tailing (V3-RS1)

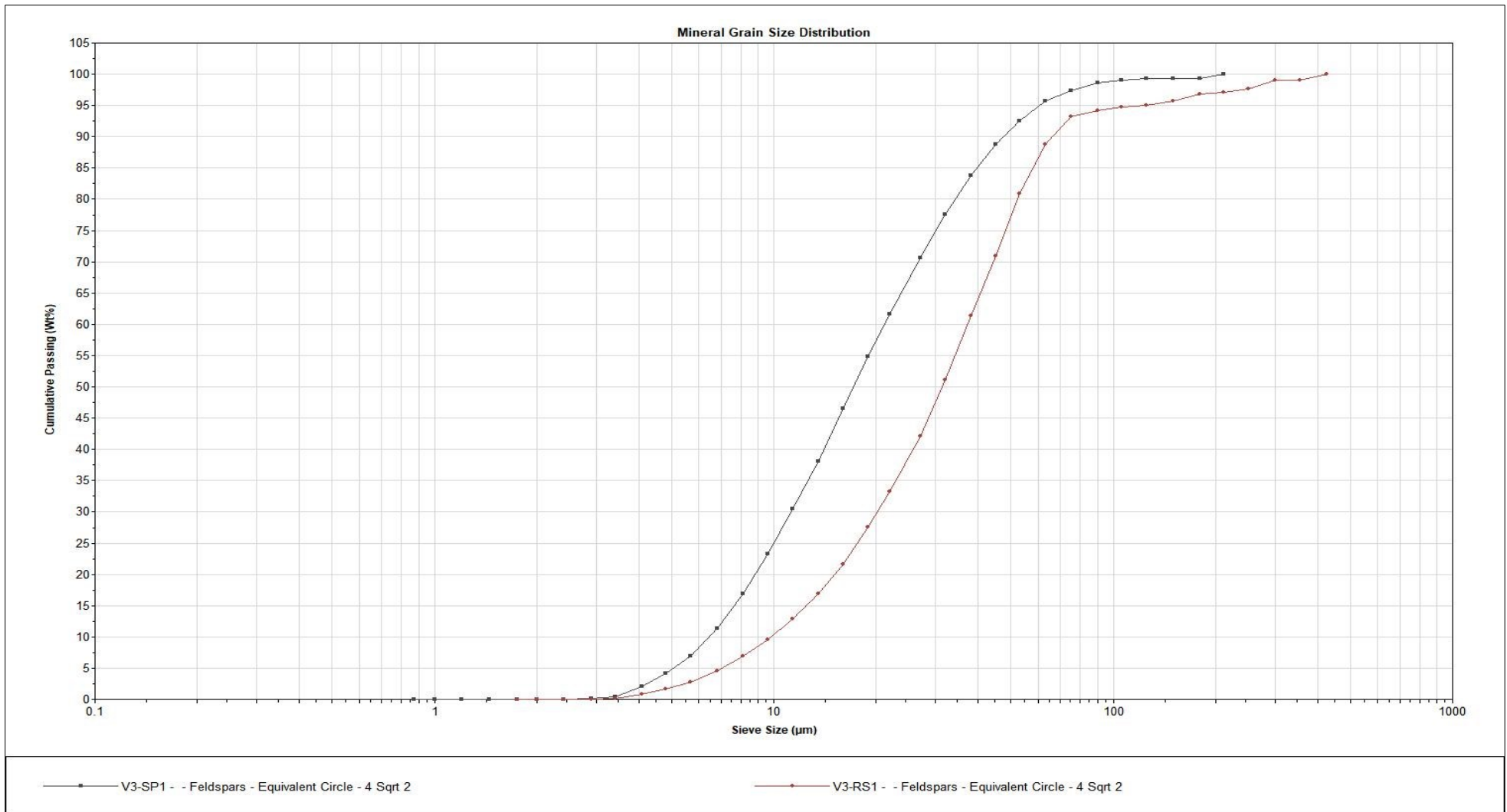


Figure 33. Grain size distribution curve for feldspar in the concentrate (V3-SP1) and the tailing (V3-RS1)

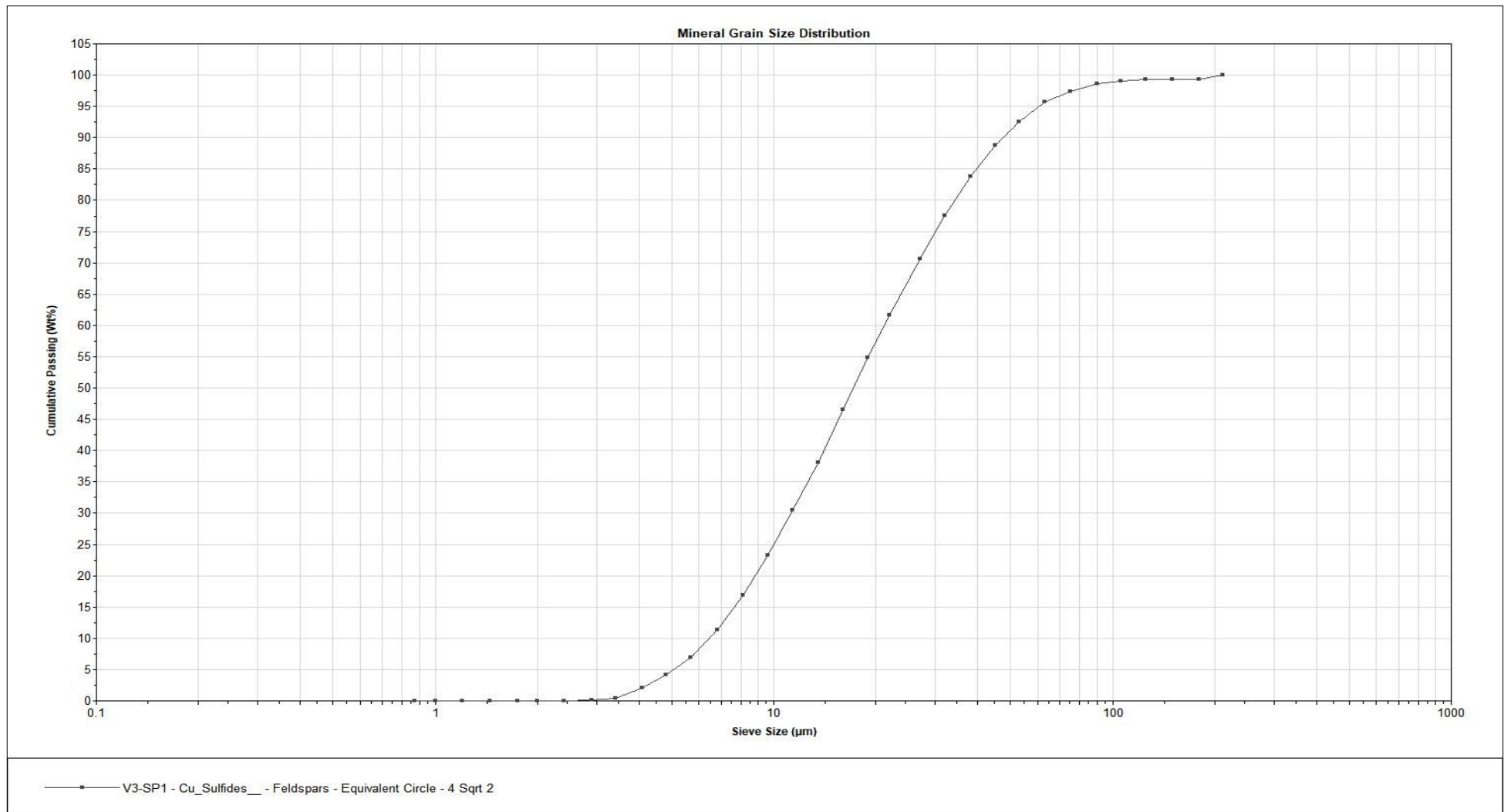


Figure 34. Grain size distribution curve for feldspar in the concentrate (V3-SP1)

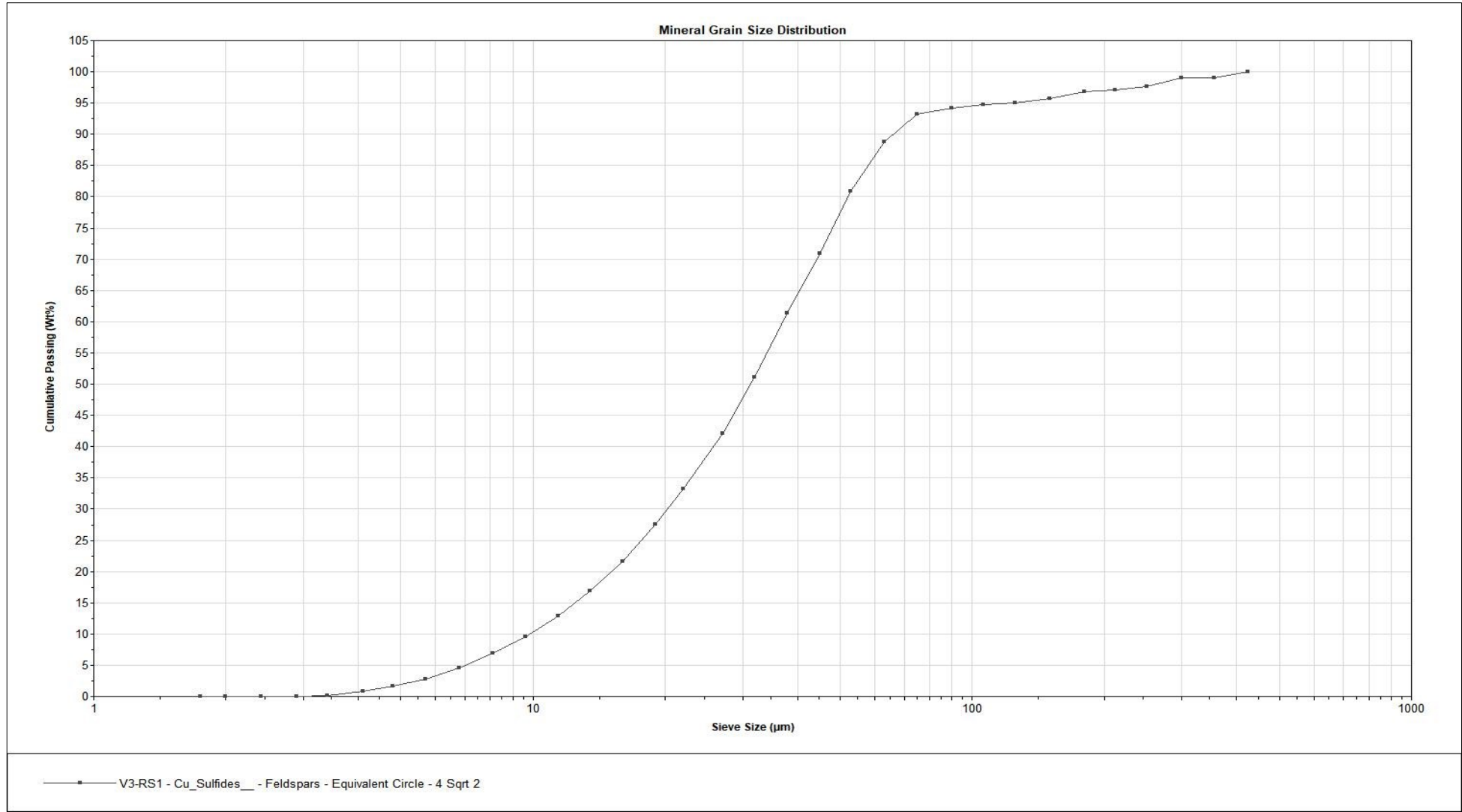


Figure 35. Grain size distribution curve for feldspar in the tailing (V3-RS1)

4.5. Grain size distribution curve for mica in both the concentrate (V3-SP1) and the tailing (V3-RS1)

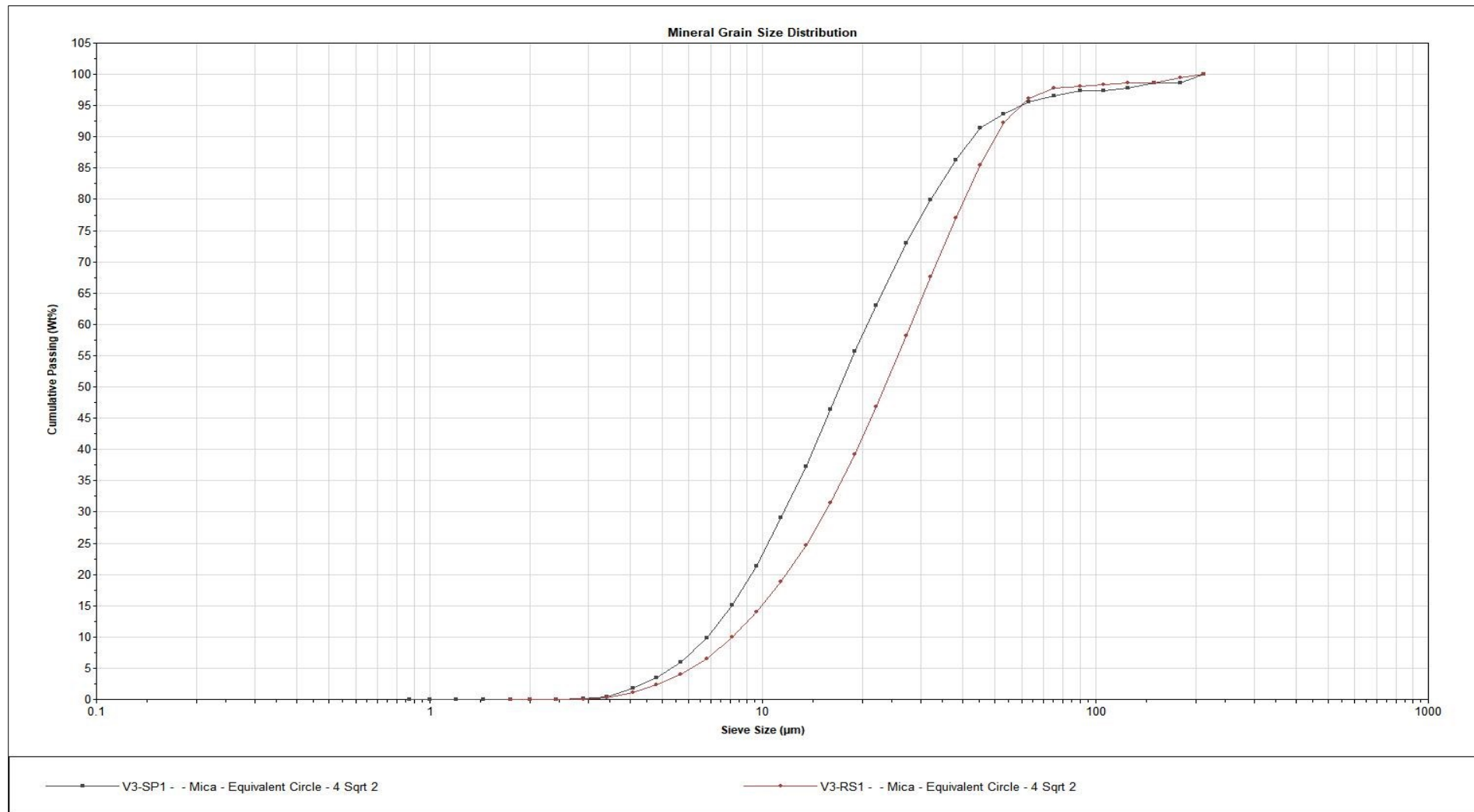


Figure 36. Grain size distribution curve for mica in the concentrate (V3-SP1) and the tailing (V3-RS1)

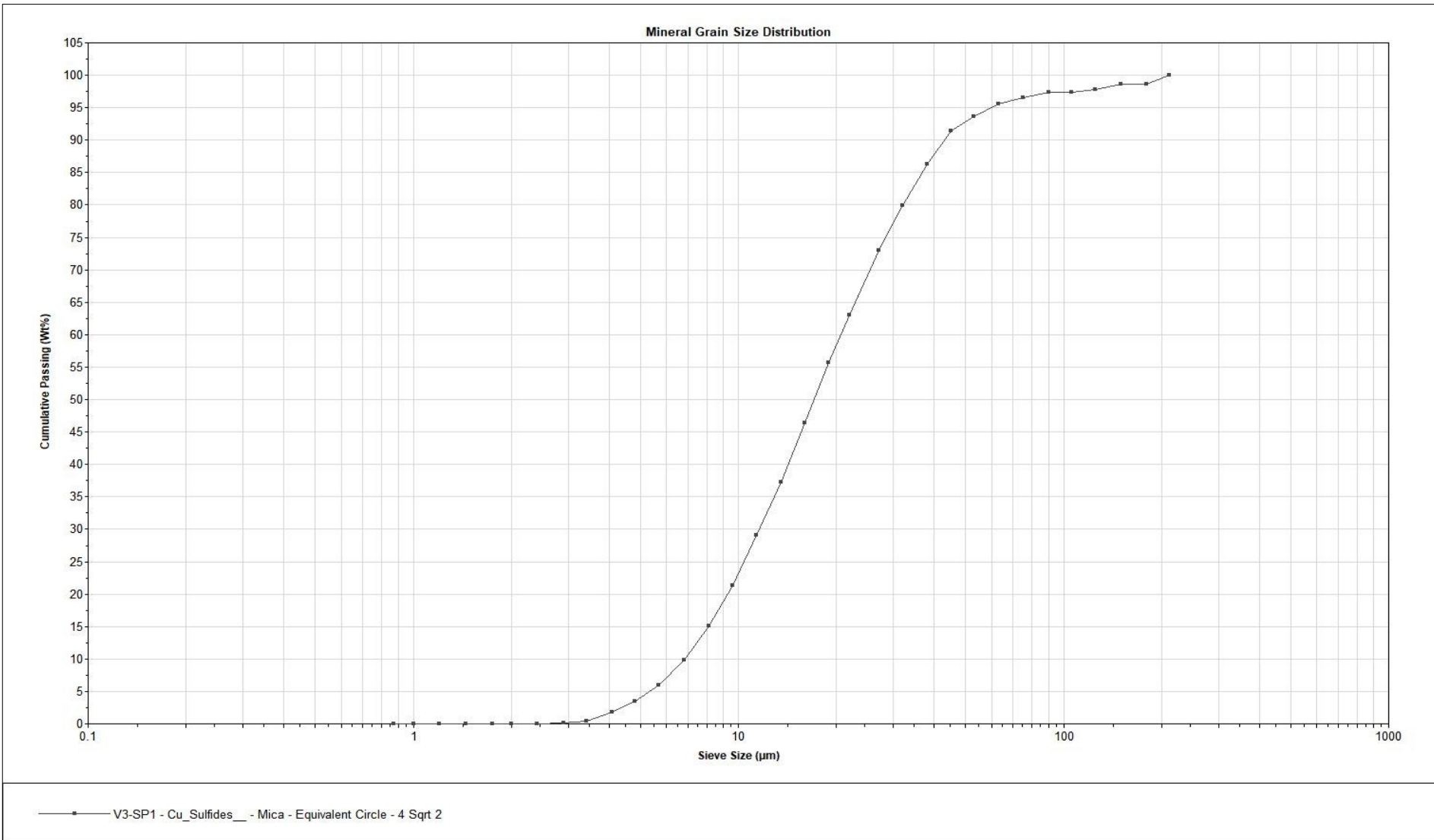


Figure 37. Grain size distribution curve for mica in the concentrate (V3-SP1)

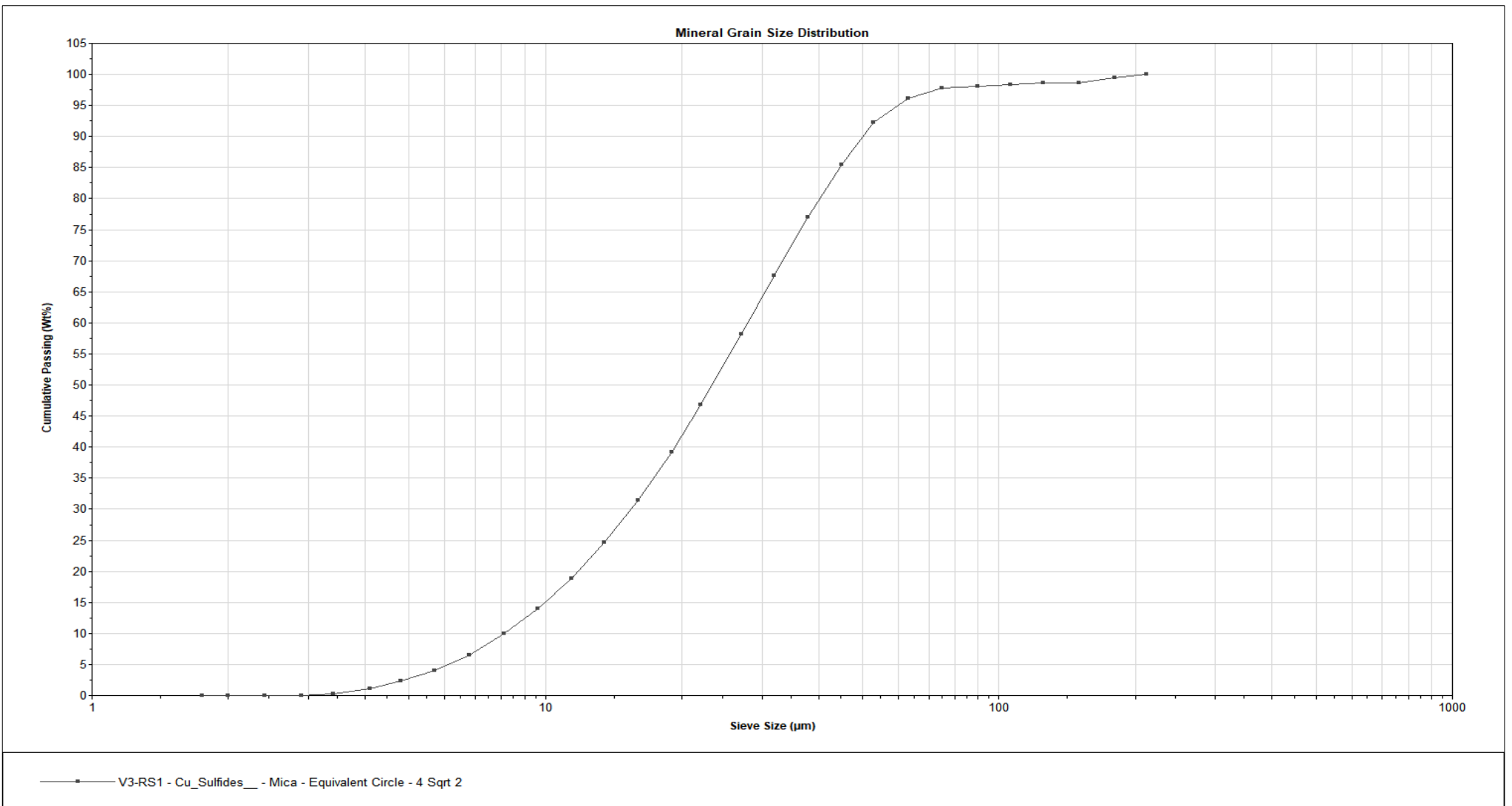


Figure 38. Grain size distribution curve for mica in the tailing (V3-RS1)

5. Preparing corresponding grain size histograms for copper minerals (grouped together), pyrite, quartz, feldspar, and mica from the concentrate.

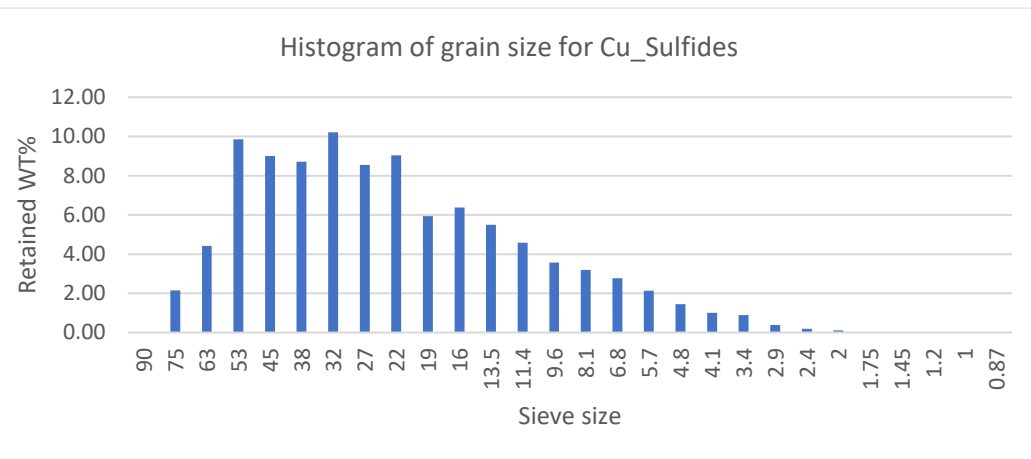


Figure 39. Cu_Sulfides grain size histogram in the concentrate V3-SP1

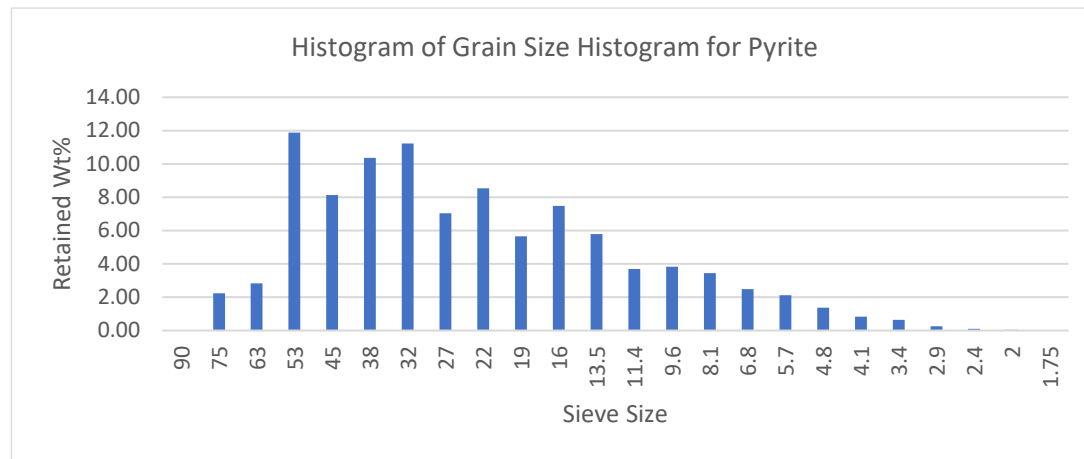


Figure 40. Pyrite grain size histogram in the concentrate V3-SP1

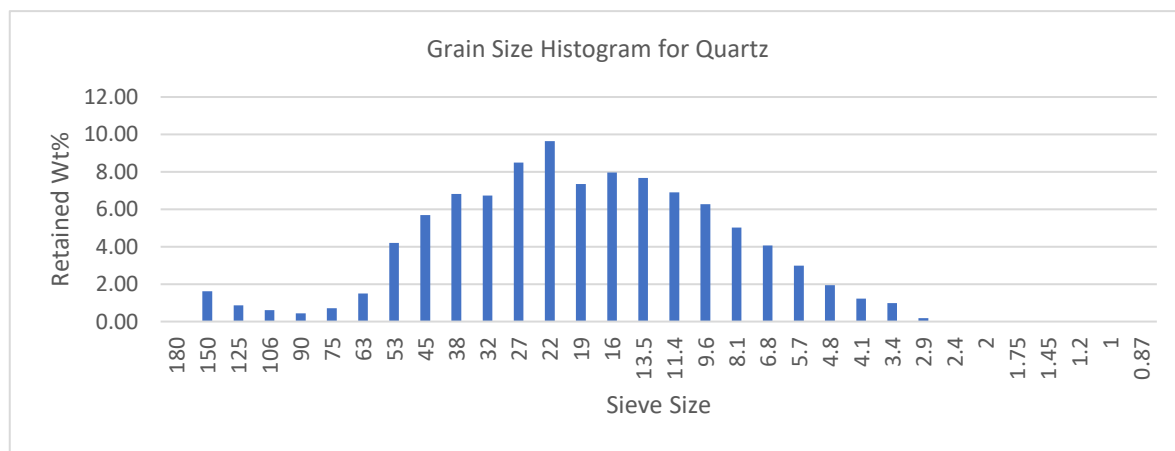


Figure 41. Quartz grain size histogram

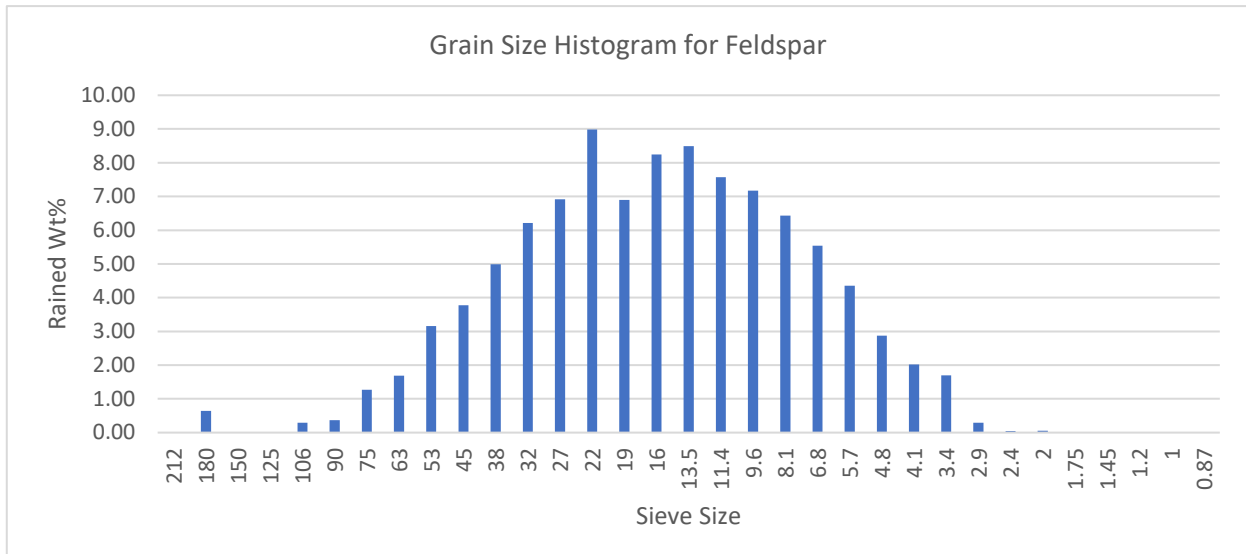


Figure 42. Feldspar grain size histogram

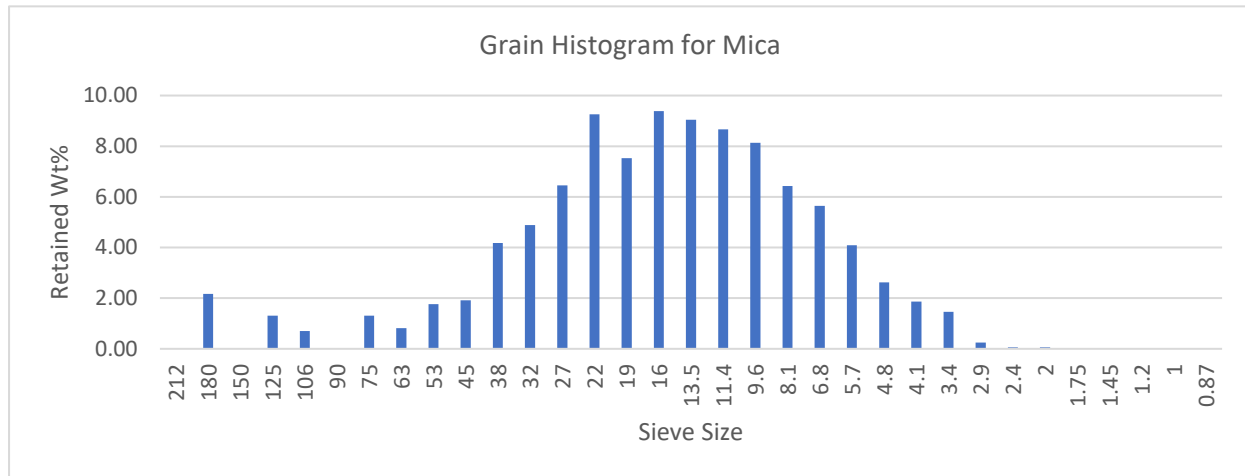


Figure 43. Mica grain size histogram

5.1. Description of the corresponding grain size histograms

The grain size distribution of copper sulfides as shown in Figure 39 shows a peak between **53 μm** and **13.5 μm**, with the highest retained weight percentage around 10%. This indicates that the majority of copper sulfides are medium to fine-grained. As for pyrite in Figure 40, the grain size distribution peaks between **53 μm** and **11.4 μm**, with a retained weight percentage of around 12%. However, the distribution sharply decreases at 6.8 μm, indicating fewer fine grains in the sample.

With regards to quartz, feldspar, and mica, the grain size distribution peaks between **53 µm** and **8.1 µm** with retained weight percentage of approximately 10%. The lowest retention is observed between **5.7 µm** and **2 µm**, indicating a lower concentration of fine grains.

6. Execution of an electronic filtering of the concentrate and tailings through EC diameter. Definition of three convenient grain size classes for this filtering by using the cumulative particle grain size distribution curve.

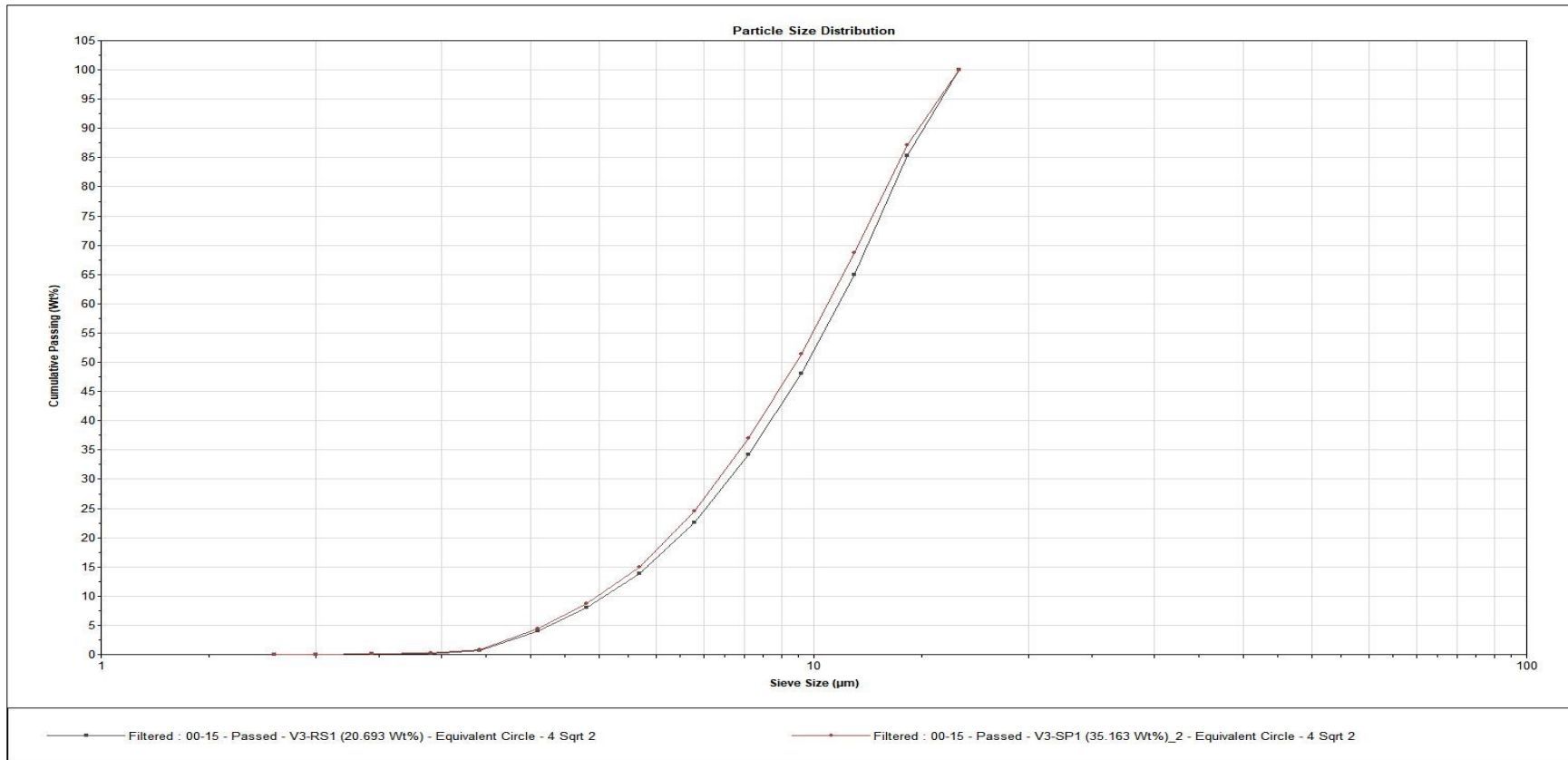


Figure 44. filtered (00-15 µm) particle size distribution curve for the concentrate (V3-SP1) and the tailing (V3-RSI)

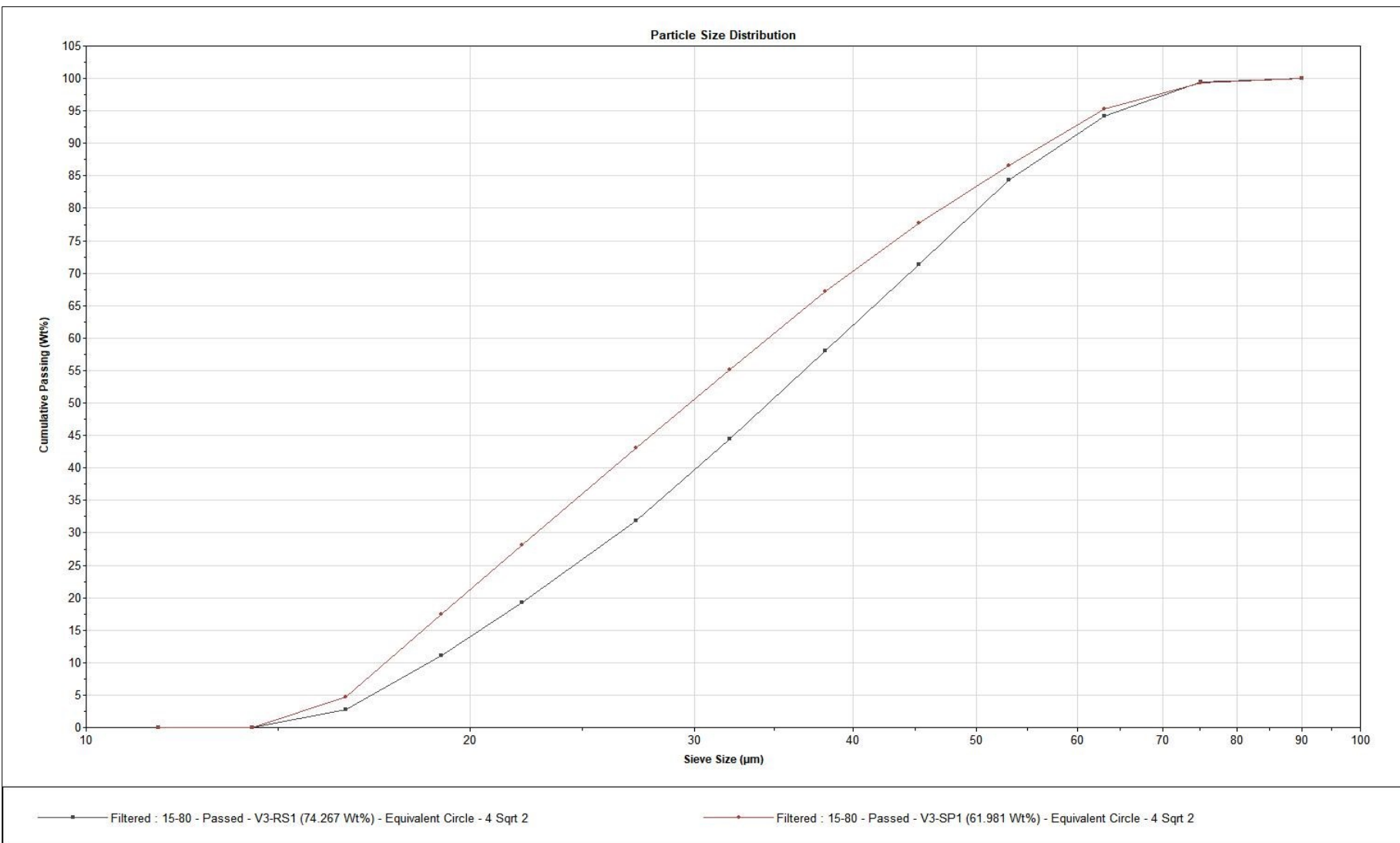


Figure 45. filtered (15-80 μm) particle size distribution curve for the concentrate (V3-SP1) and the tailing (V3-RS1)

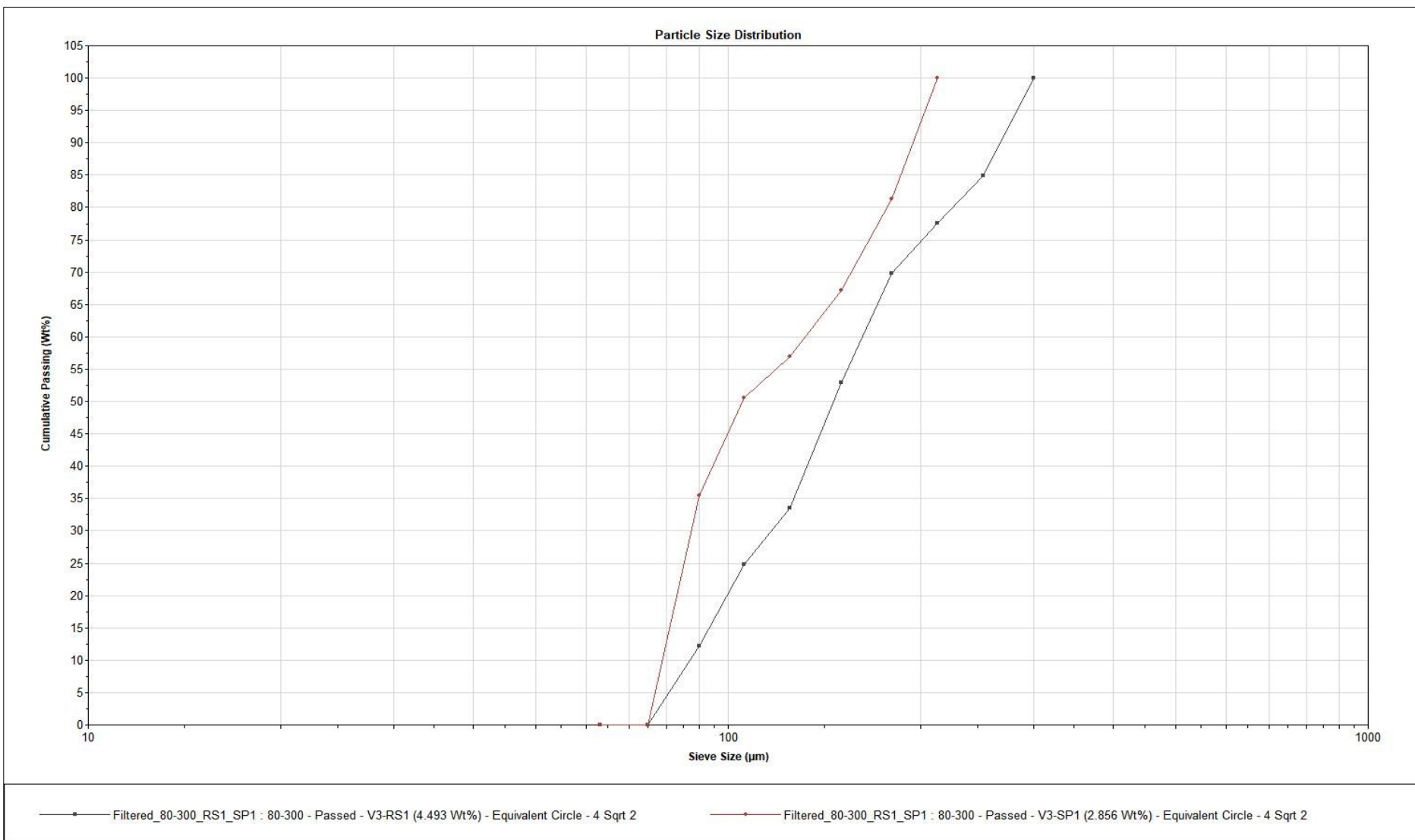


Figure 46. filtered (80-300 μm) particle size distribution curve for the concentrate (V3-SP1) and the tailing (V3-RS1)

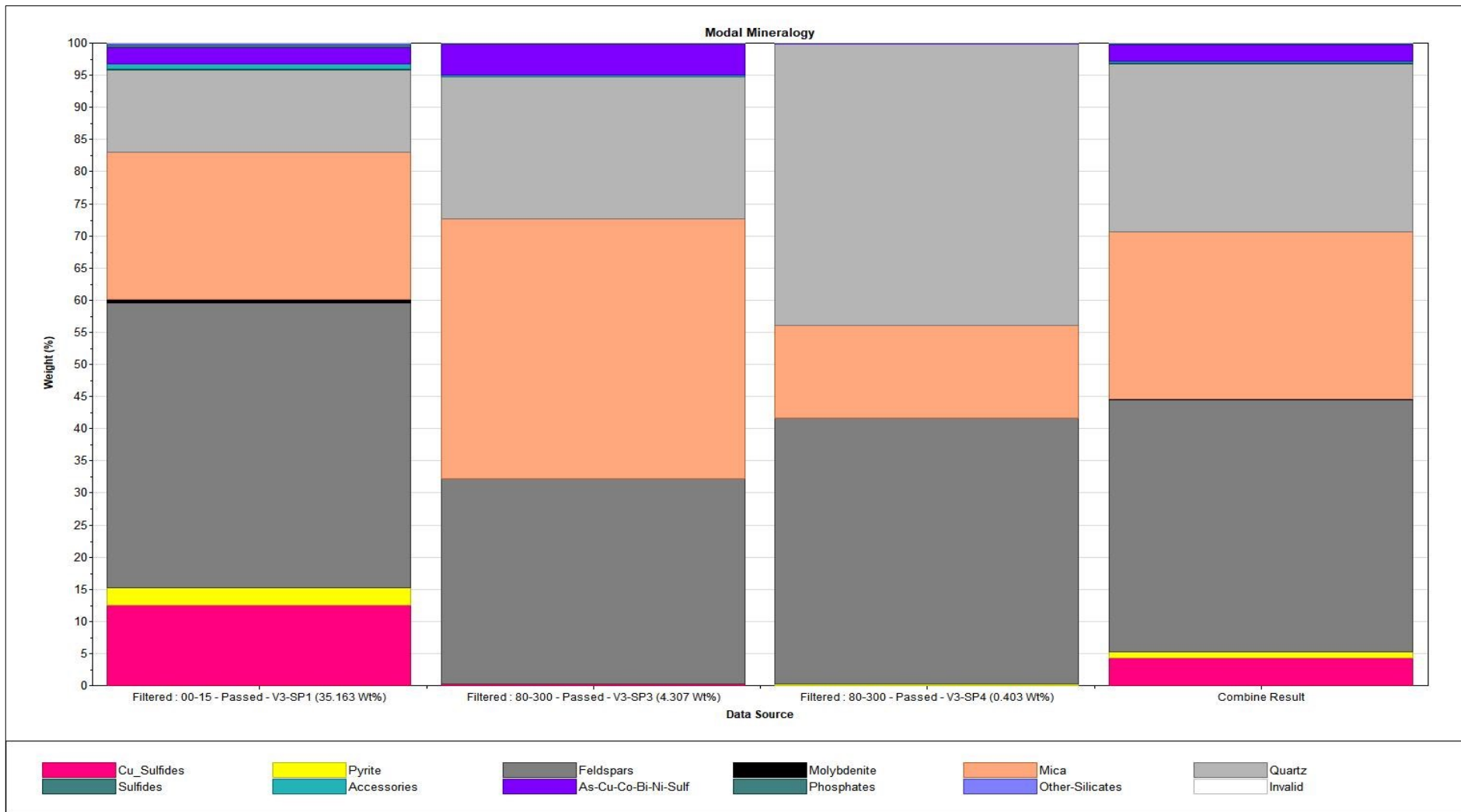


Figure 47. Filtered (00-15 μm ; 80-300 μm) modal mineralogy for V3-SP1; V3-SP3; V3-SP4

7. Giving a text with a comparative description of modes and mineral liberation (Particle Composition and Free Surface) of unfiltered and filtered subsamples from all samples.

7.1. Mineral liberation by particle composition

Mineral liberation by particle composition help assess how mineral are separated based on particle size and composition. Key aspects include the efficiency of separation, the degree of liberation, and its impacts on processing methods. Proper liberation improves recovery rates and enhances final product quality. **Figure 48** illustrates the liberation of copper sulfides across different unfiltered concentrates at 85-90% liberation class. In concentrate (V3-SP1), copper sulfide liberation ranges from **93% to 96%**. In concentrate (V3-SP3), it is approximately **83% to 88%**, while concentrate (V3-SP4) shows a liberation of **85% to 90%**. As for the tailing (V3-RS1), the liberation of copper sulfides is around 83 weights %.

Figure 49 shows the effectiveness of copper sulfide liberation across different filtered samples filtered at 00-15 μm . The liberation efficiency is around **95%** in the **85-90%** liberation class. For concentrate (V3-SP3), **90% to 92%** of copper sulfides are recovered within the **90-95%** liberation class. In concentrate (V3-SP4), liberation occurs at **85-90%** liberation class with an effectiveness of **96** weights %. In contrast, the tailing shows nearly **100%** liberation of copper sulfides. **Figure 50** illustrates the effectiveness of copper sulfide liberation filtered at 15-80 μm . The liberation from concentrate (V3-SP1) is **90-93%**, while it is **65-75%** from concentrate (V3-SP3). Conversely, concentrate (V3-SP4) shows a recovery of **86-90%**, compared to **81-82%** from the tailing.

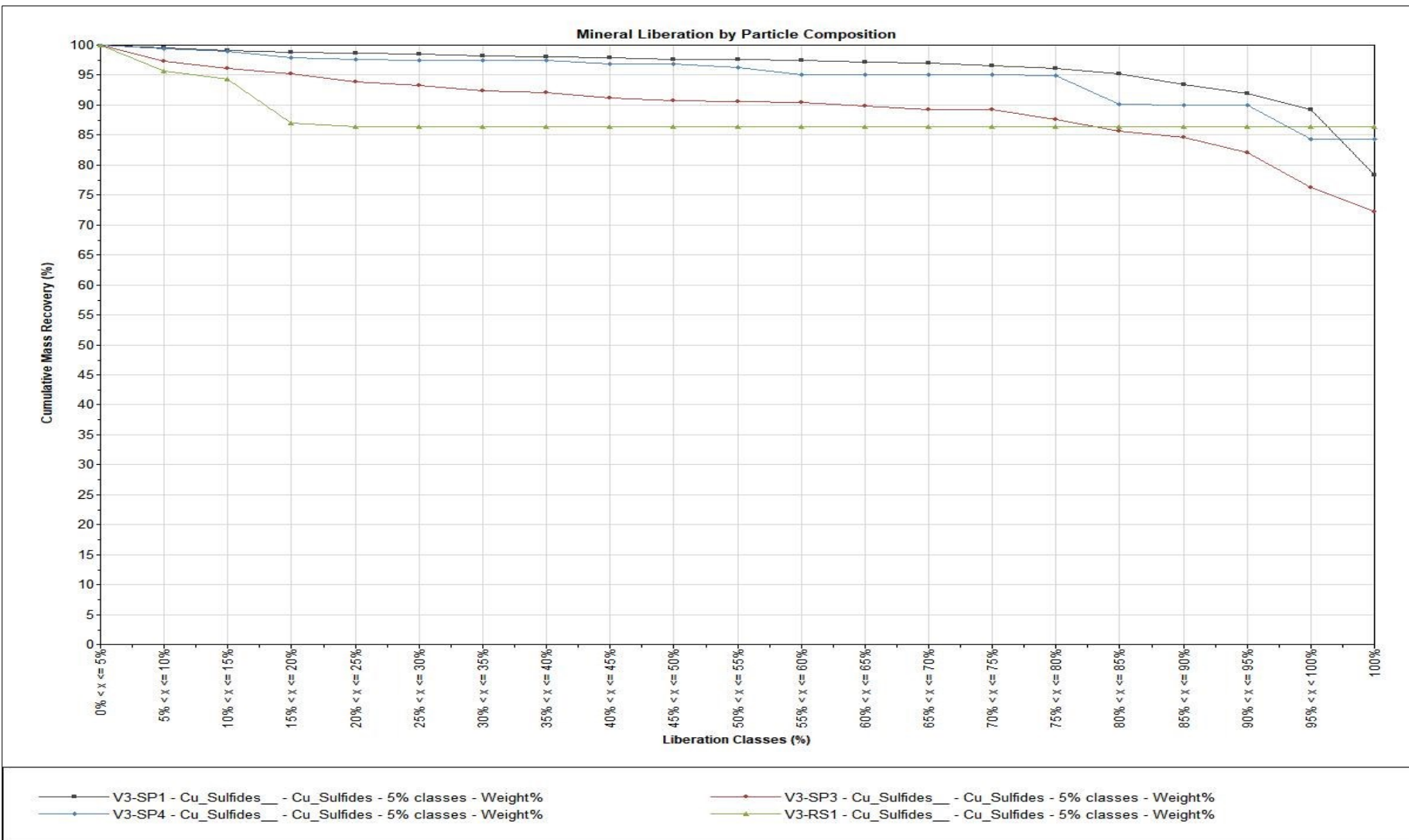


Figure 48. Unfiltered mineral liberation by particle composition with samples, including V3-SP1, V3-SP3, V3-SP4, V3-RS1

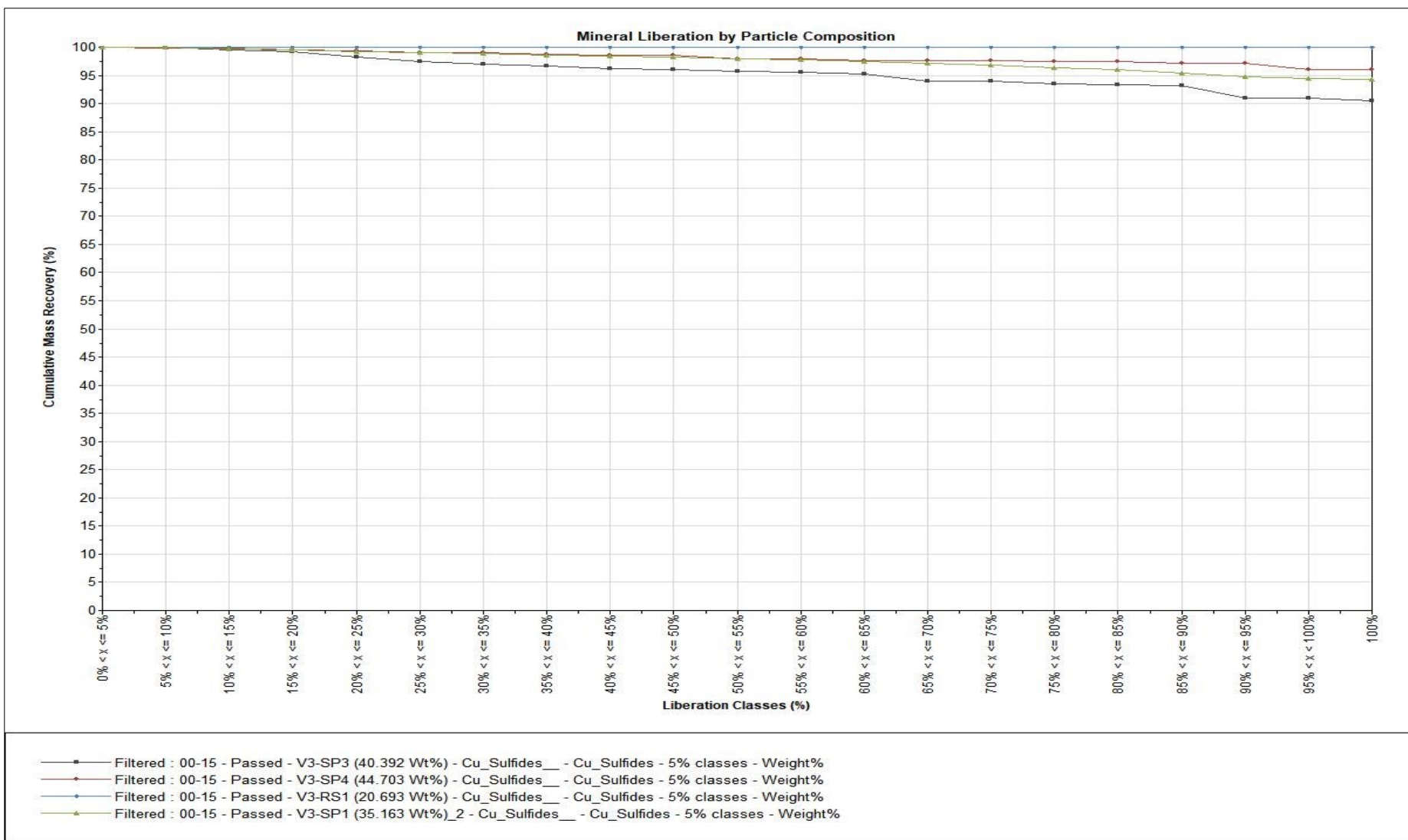


Figure 49. mineral liberation by particle composition with samples, including V3-SP1, V3-SP3, V3-SP4, V3-RS, filtered at 00-15 μm

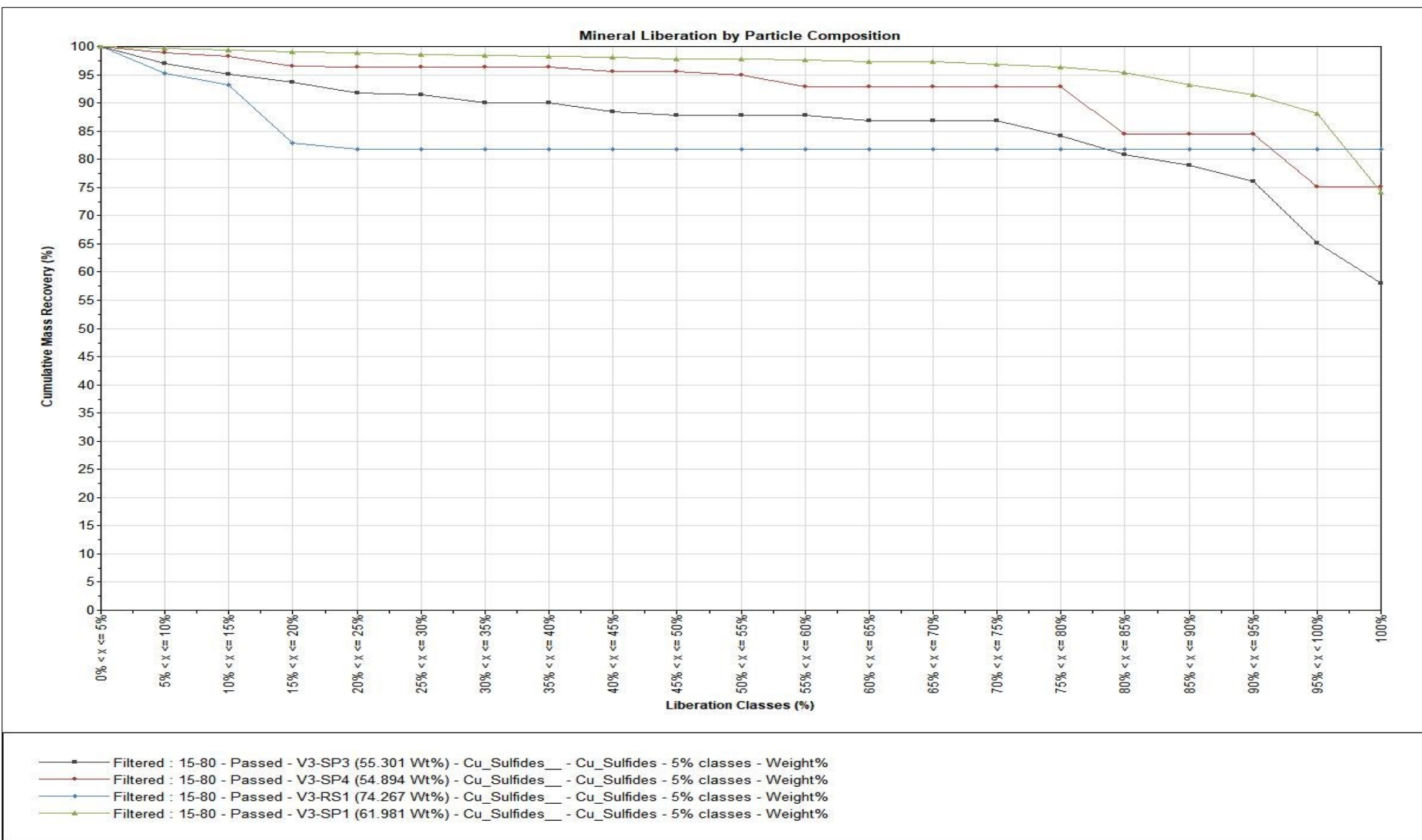


Figure 50. mineral liberation by particle composition with samples, including V3-SP1, V3-SP3, V3-SP4, V3-RS, filtered at 15-80 μm

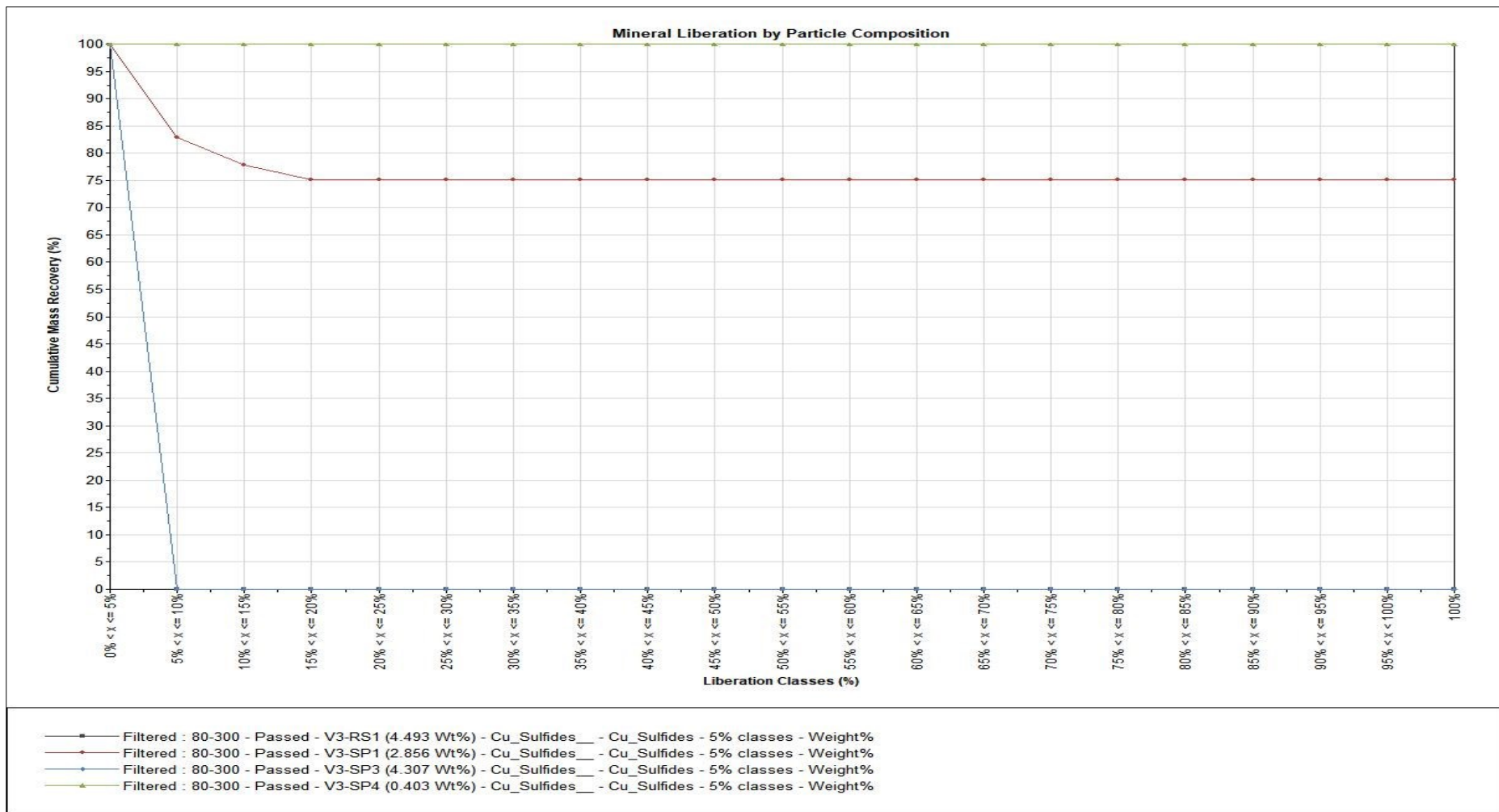


Figure 51. mineral liberation by particle composition with samples, including V3-SP1, V3-SP3, V3-SP4, V3-RS, filtered at 80-300 μm

Figure 51 shows the copper sulfide liberation by particle composition for the four samples filtered at 80-300 μm . The results reveal notable variations in liberation percentages among the samples. The concentrate V3-SP4 shows the highest liberation rate, starting at nearly 100% in the lower liberation classes and remaining above the other samples throughout, indicating higher liberation. As for the concentrate V3-SP1, the liberation percentage remains relatively stable, ranging between 70-80% across the liberation classes, showing moderate liberation efficiency. In addition, the concentrate V3-SP3 exhibits a steeper decline in liberation, indicating less effective liberation compared to V3-SP4. On the other hand, the concentrate V3-RS1 is almost negligible, reflecting very low liberation, characteristics of a tailing sample. In conclusion, V3-SP4 demonstrates the most effective copper sulfide liberation, while V3-SP1 and V3-SP3 show moderate liberation. V3-RS1 displays minimal liberation, as expected for a tailing sample.

7.2. Mineral liberation by particle surface

Particle liberation by surface refers here to the degree to which minerals are freed from the surrounding matrix based on the surface area. Effective liberation improves separation efficiency in processing, as larger surface areas facilitate better contact with reagents or physical separation methods. This process can be crucial for optimizing recovery rates and enhancing the quality of the final product.

Figure 51 shows the liberation of copper sulfides based on free surface area across different unfiltered samples, including V3-SP1, V3-SP3, V3-SP4, and V3-RS1. It shows that, within the **85-90%** liberation class, **84-90%** of copper sulfides are liberated from concentrates V3-SP1 and V3-SP4, while approximately **75%** is liberated from concentrate V3-SP3. In contrast, copper sulfide liberation reaches **86%** in the sample V3-RS1. In addition, Figure 52 illustrates copper sulfide liberation by free surface area filtered at 00-15 μm . At the **85-90%** liberation class, **92%** of copper sulfides are liberated from concentrate V3-SP1, and **91%** from concentrate V3-SP3. For concentrate V3-SP4 and tailing V3-RS1, the liberation by free surface is approximately **97%** and **100%**, respectively.

Figure 53 presents copper sulfide liberation by free surface area filtered at 15-80 μm . In the **85-90%** liberation class, **87 weights %** of copper sulfides are liberated from concentrate V3-SP1, while **59 weights %** are liberated from concentrate V3-SP3. Concentrate V3-SP4 shows a liberation of **84 weights %**, and tailing V3-RS1 exhibits a liberation of **82 weights %**.

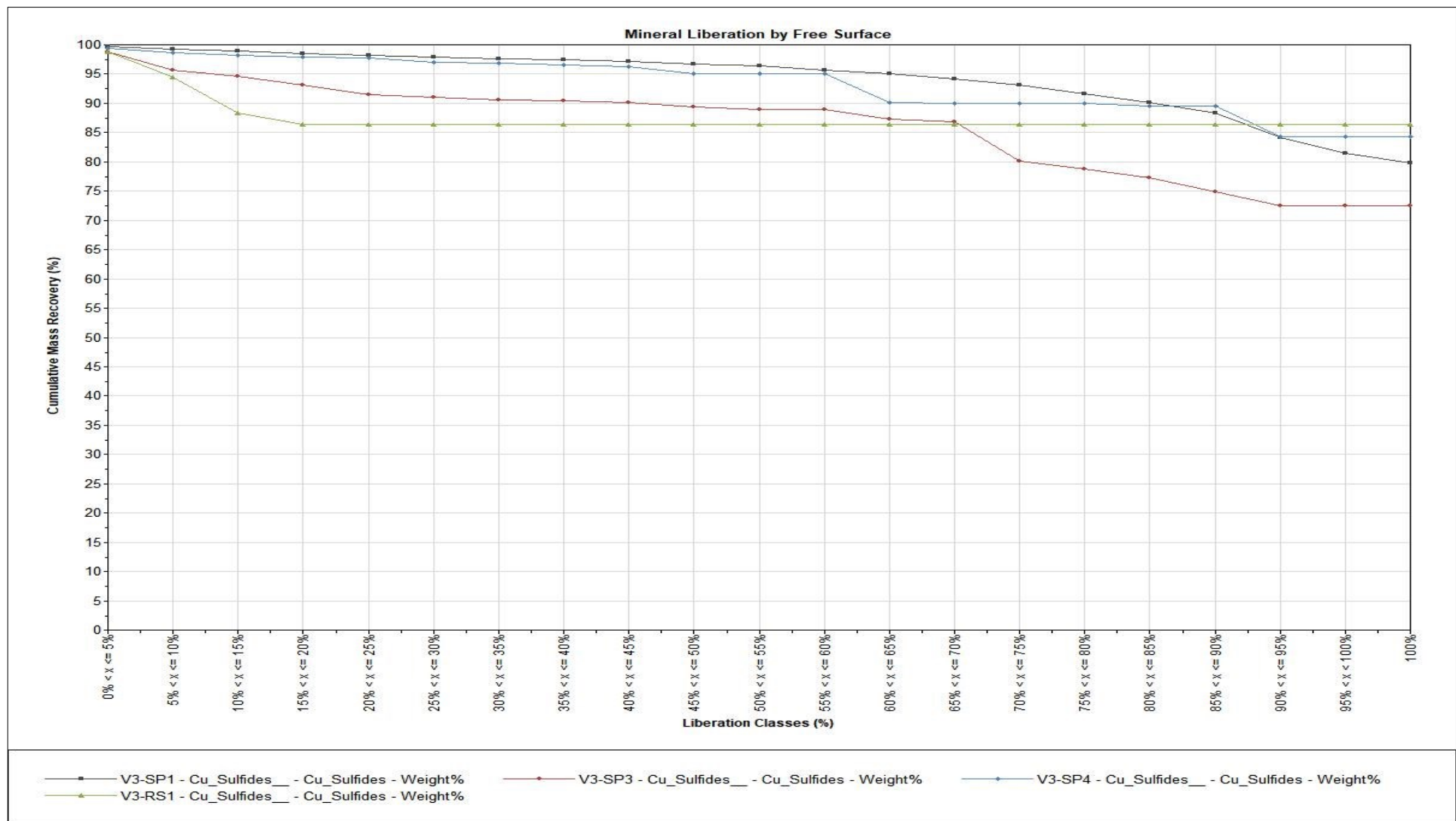


Figure 52. Unfiltered mineral liberation by free surface with samples, including V3-SP1, V3-SP3, V3-SP4, V3-RS1

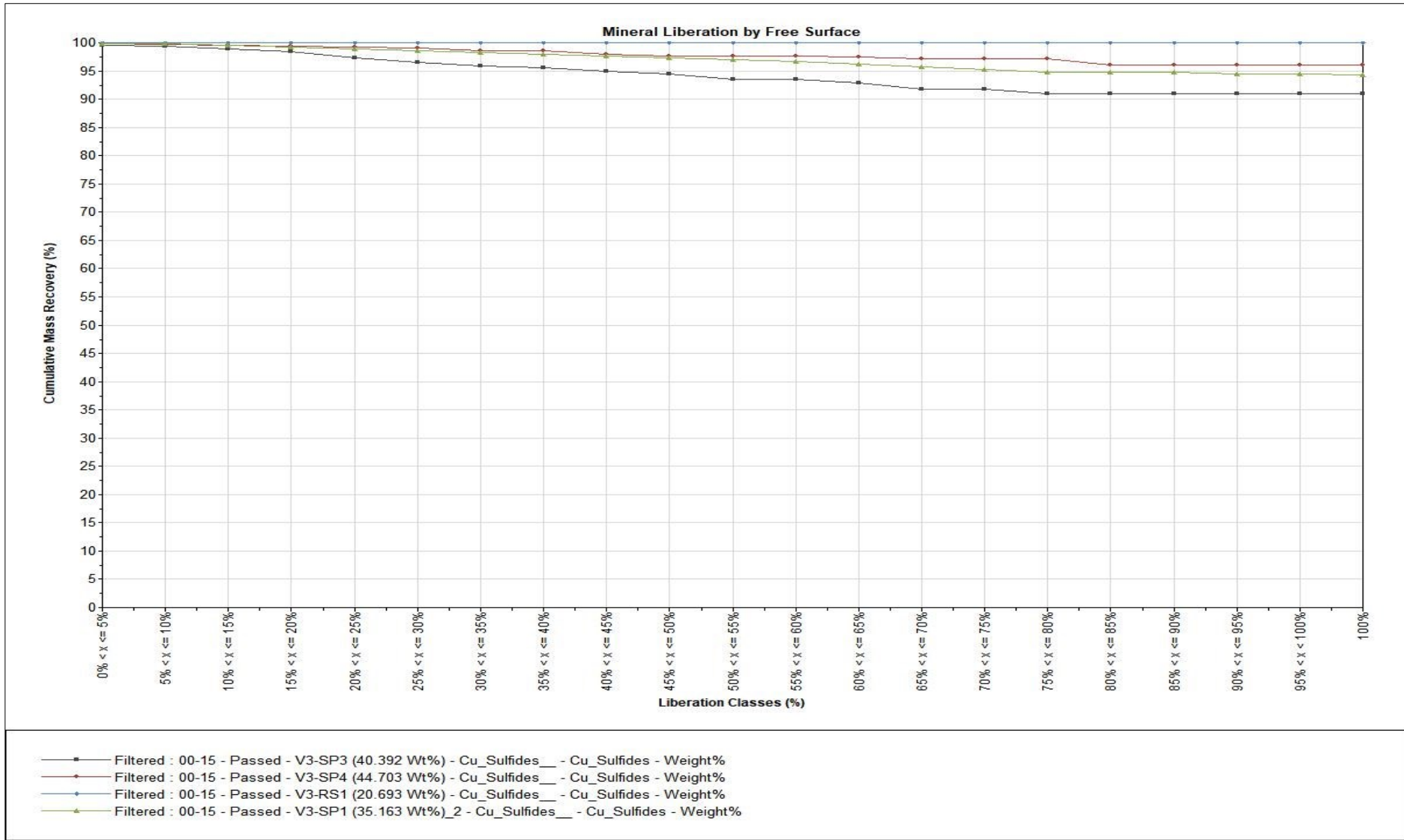


Figure 53. Mineral liberation by free surface with samples, including V3-SP1, V3-SP3, V3-SP4, V3-RS1 filtered at 00-15 μm

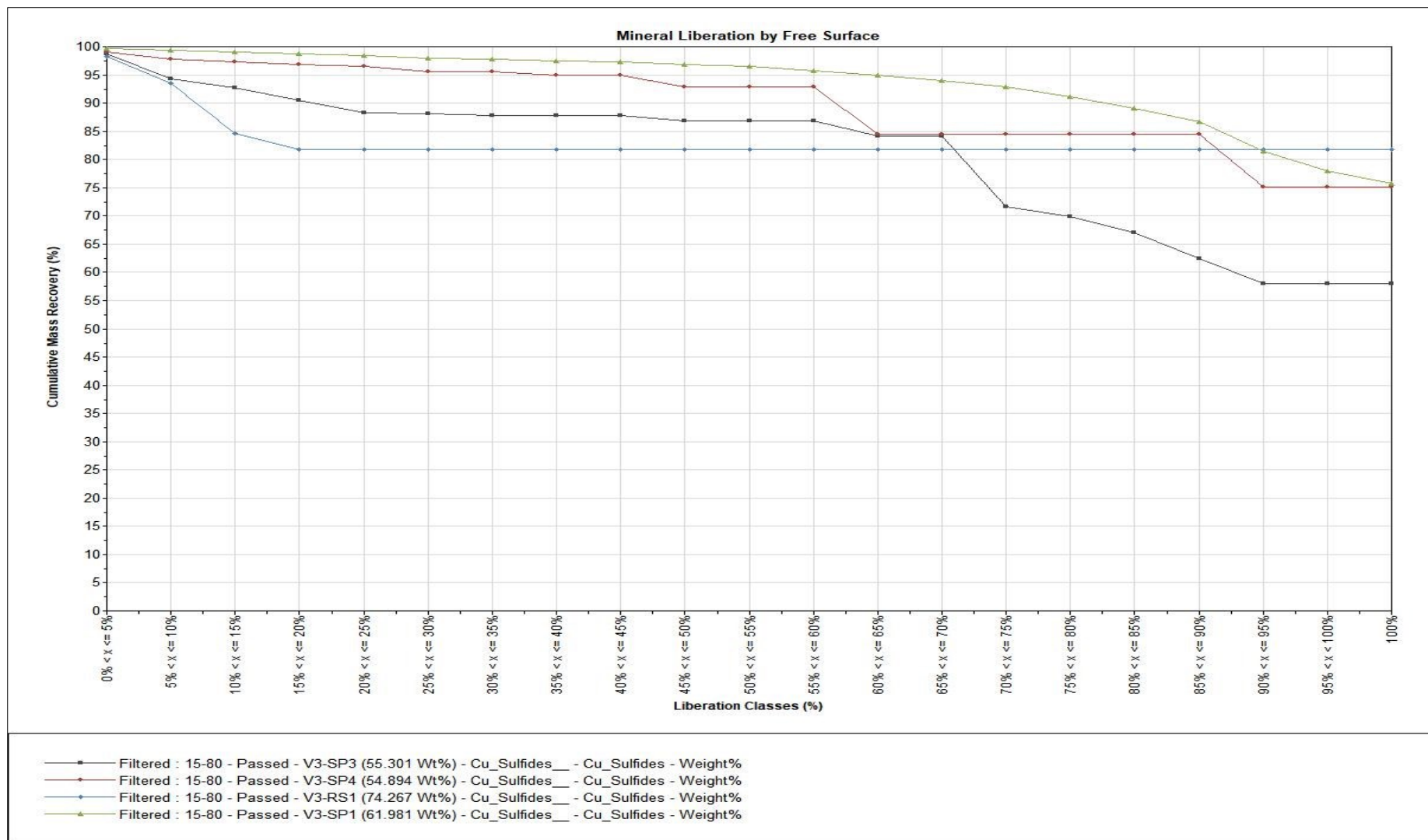


Figure 54. Mineral liberation by free surface with samples, including V3-SP1, V3-SP3, V3-SP4, V3-RS1 filtered at 15-80 μm



Figure 55. Mineral liberation by free surface with samples, including V3-SP1, V3-SP3, V3-SP4, V3-RS1 filtered at 80-300 μm

Figure 55 illustrates the copper sulfides liberation by free space for the four samples filtered at 80-300 μm . The results revealed that the concentrate V3-SP4 maintains a steady high liberation, remaining flat across the liberation class range, while V3-SP1 shows a consistent liberation at about 80% across the liberation classes. However, V3-SP3 experiences a decrease as the liberation class increases. With regards to V3-RS1, it shows the lowest performance with a liberation starting near 95% and quickly dropping as the liberation classes progress.

8. Reference

- Chen, Xumeng, Yongjun Peng, and Dee Bradshaw. 2014. "The Separation of Chalcopyrite and Chalcocite from Pyrite in Cleaner Flotation after Regrinding." *Minerals Engineering* 58:64–72. doi: <https://doi.org/10.1016/j.mineng.2014.01.010>.
- Hermo, Ma. Isabella, Maria Ines Rosana Balangue-Tarriela, Ryohei Takahashi, Jillian Aira Gabo-Ratio, and Sofia Marah Frias. 2022. "Mineralization Styles and Ore-Forming Conditions of the Quartz-Fragment-Rich Breccia (QBX) at the Didipio Alkalic Porphyry Cu-Au Deposit, Nueva Vizcaya, Philippines." *Ore Geology Reviews* 143:104724. doi: <https://doi.org/10.1016/j.oregeorev.2022.104724>.
- Kavalieris, Imants, Khashgerel B, Leah Morgan, Alexander Undrakhtamir, and Adiya Borohul. 2017. "Characteristics and $^{40}\text{Ar}/^{39}\text{Ar}$ Geochronology of the Erdenet Cu-Mo Deposit, Mongolia." *Economic Geology* 112:1033–53. doi: 10.5382/econgeo.2017.4500.
- Sillitoe, R. H. 2010. "Porphyry Copper Systems." *Economic Geology* 105(1):3–41. doi: 10.2113/gsecongeo.105.1.3.
- Zhao, Jing, Joël Brugger, Guorong Chen, Yung Ngothai, and Allan Pring. 2014. "Experimental Study of the Formation of Chalcopyrite and Bornite via the Sulfidation of Hematite: Mineral Replacements with a Large Volume Increase." *American Mineralogist* 99(2–3):343–54. doi: 10.2138/am.2014.4628.